Delft University of Technology

An optimisation approach for planning preventive drought management measures

Paez-Trujillo, Ana M.; Hernandez-Suarez, J. Sebastian; Alfonso, Leonardo; Hernandez, Beatriz; Maskey, Shreedhar; Solomatine, Dimitri

Important note
To cite this publication, please use the final published version (if applicable).
Please check the document version above.

An optimisation approach for planning preventive drought management measures

Ana M. Paez-Trujillo [a,b,d,*], J. Sebastian Hernandez-Suarez [c], Leonardo Alfonso [a], Beatriz Hernandez [d], Shreedhar Maskey [a], Dimitri Solomatine [a,b,e]

[a] IHE Delft Institute for Water Education, P.O. Box 3015, 2601 DA Delft, the Netherlands
[b] Delft University of Technology, Water Resources Section, P.O. Box 5048, 2600 GA Delft, the Netherlands
[c] Department of Civil and Environmental Engineering, Universidad de los Andes, Carrera 1 Este # 19A – 40 ML-714, Bogota, Colombia
[d] Fundación Natura Colombia, Carrera 21 No. 39–43, Bogotá, Colombia
[e] Water Problems Institute of RAS, 119333, Gubkina 3, Moscow, Russia

HIGHLIGHTS

- Preventive drought management measures can reduce the severity of droughts.
- Allocating drought management measures is a multi-objective problem.
- This study uses an optimisation approach to allocate drought management measures.
- Management measures' effect on droughts exhibits temporal and spatial variations.
- Management measures show contrasting impacts on different types of droughts.

GRAPHICAL ABSTRACT
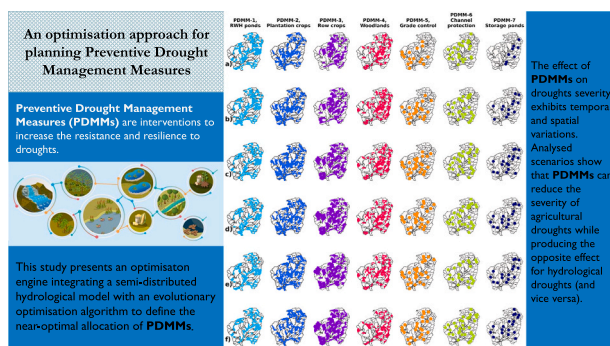
ARTICLE INFO

ABSTRACT

While drought impacts are widespread across the globe, climate change projections indicate more frequent and severe droughts. This underscores the pressing need to increase resistance and resilience to drought. The strategic application of Preventive Drought Management Measures (PDMMs) is a suitable avenue to reduce the likelihood of drought and ameliorate associated damages. In this study, we use an optimisation approach with a multi-criteria decision-making method to allocate PDMMs for reducing the severity of agricultural and hydrological droughts. The results indicate that implementing PDMMs can reduce the severity of agricultural and hydrological droughts, and the obtained management scenarios (solutions) highlight the utility of multi-objective optimisation for PDMMs planning. However, examined management scenarios also illustrate the trade-off between managing agricultural and hydrological droughts. PDMMs can alleviate the severity of agricultural droughts while producing opposite effects for hydrological droughts (or vice versa). Furthermore, the impact of PDMMs displays temporal and spatial variabilities. For instance, PDMMs implementation within a specific subbasin may mitigate the severity of one type of drought in a given month yet exacerbate drought conditions in preceding or subsequent months. In the case of hydrological droughts, the PDMMs may intensify streamflow deficits in the

intervened subbasins while alleviating the hydrological drought severity downstream (or vice versa). These complexities emphasise a customised implementation of PDMMs, considering the basin characteristics (e.g., rainfall distribution over the year, soil properties, land use, and topography) and the quantification of PDMMs' effect on the severity of each type of drought.

1. Introduction

Drought, directly and indirectly, impacts society, the environment and the economy (Duel et al., 2022; UNDRR, 2021; Vogt et al., 2018). Direct impacts result from the interaction between water deficit and social, economic or environmental components and are observed in drought-affected areas (UNDRR, 2021; Vogt et al., 2018). These impacts include limited water supplies, crop loss, wetland drying, and reduced energy production. Indirect consequences relate to secondary effects on natural or economic resources and can be observed in areas far away from where the drought originated and continue long after the drought has ended (UNDRR, 2021; Vogt et al., 2018). Indirect consequences can impact biodiversity and food prices and, in extreme cases, may affect human health and result in loss of income and food insecurity (UNDRR, 2021).

Extensive drought impacts and climate change projections showing more frequent and severe droughts worldwide highlight the pressing need to develop drought management plans (Carrão et al., 2018; Cottrell et al., 2019; Haile et al., 2020; UNCCD, 2022; Vicente-Serrano et al., 2020). Literature on drought management stresses the importance of proactive drought management (FAO, 2019; Gerber and Mirzabaev, 2017; Wilhite, 2016). This approach does not respond to specific events but recognises drought planning as a permanent and continuing need. Proactive drought management aims to create resistance and resilience to droughts, minimising negative impacts in advance and relies on three pillars: 1) drought monitoring and early warning systems, 2) drought risk and vulnerability assessment, 3) drought preparedness and mitigation (Pischke and Stefanski, 2017; Tsegai et al., 2018; Wilhite, 2019). Particularly, the third pillar of proactive drought management refers to measures to mitigate the potential negative of droughts and to enable ecosystems and communities to withstand the effects of droughts more effectively (Wilhite, 2019). These measures can be grouped into four categories according to their purpose: preventive or strategic, operational, organisational and restoration (Global Water Partnership Central and Eastern Europe, 2015). They vary broadly, e.g. from interventions at the field level applied before the drought occurs to negotiated global compensation for damage to land due to droughts (Assimacopoulos et al., 2015; King-Okumu, 2021; World Bank, 2019). This study analyses preventive drought management measures (PDMMs) applied at the basin level.

PDMMs are developed prior to the onset of droughts. At the basin level, PDMMs encompass multiple management actions for different land use types (King-Okumu, 2021; Sanz et al., 2017; Sayers et al., 2017; UNCCD, 2019). Interventions can be intended for water bodies, flood-plains and wetlands restoration; croplands soil conservation and best management practices (terracing, mulching, cover crops), water harvesting and recharge; forest and woodlands conservation, reforestation and agroforestry; and agropastoralism for mixed land uses.

Overall, modelling and field studies on PDMM focus on one specific measure. Assessment of measures' performance mainly relies on interventions' effectiveness in increasing infiltration and water availability, improving soil water-holding capacity and preventing land degradation or desertification (Basche, 2017; Beets and Beets, 2020; Oweis et al., 2012; Sanz et al., 2017; Wambura et al., 2018; Yadav et al., 2018). While these criteria provide relevant insights into the measures' applicability for drought management, there is a lack of information on the water deficit reduction during drought periods and measures' contribution to drought alleviation is not explicitly appraised.

Application of drought mitigation measures in a consistent and

structured way has the potential to limit the negative impact of droughts on society, the environment and the economy (Global Water Partnership Central and Eastern Europe, 2015). Nevertheless, planning mitigation measures at the basin scale is not a trivial task. In a given region, a collection of measures, sites, scales, and possible configurations suitable for drought management exists. In addition, measures appropriate for reducing one type of drought may adversely impact another type of drought, e.g. agricultural drought management measures may exacerbate hydrological drought conditions. This conflict can be explained by the fact that alleviating agricultural droughts requires storing water in the soil profile, implying a reduction in rivers' discharge, increasing, in turn, hydrological droughts (Cai et al., 2015). Accordingly, selecting a right set of drought management measures is effectively a multi-objective problem.

Several multi-objective optimisation frameworks have been applied to optimise types and allocation of management strategies to improve water quality and stream health (Deb et al., 2023; Geng et al., 2019; Liu et al., 2019; Raschke et al., 2021; Zhang et al., 2023), flood management and water availability (Lewis and Randall, 2017; Liu et al., 2023; Woodward et al., 2014), or prevent soil degradation (Hildemann et al., 2023; Naseri et al., 2021; Wu et al., 2018). Regarding drought preparedness and PDMMs planning, Cai et al. (2015) developed a multi-objective stochastic optimisation model to identify the optimal combination of preventive and tactical measures under different future climate scenarios. Particularly, they provided relevant information on the required investments to mitigate drought damage and identified the trade-off between managing agricultural and hydrological droughts. In their study, the effects of the preventive measures on drought characteristics (intensity, duration, frequency) were not evaluated.

This study uses an optimisation approach to define near-optimal drought management scenarios (sets of different PDMMs combinations and allocations), estimate their impact on the severity of agricultural and hydrological droughts and analyse the trade-off between managing both types of droughts. Accordingly, we develop an optimisation engine integrating a semi-distributed hydrological model – the Soil Water Assessment Tool (SWAT) (Neitsch et al., 2011). – with an evolutionary optimisation algorithm – the Unified Non-dominated Sorting Genetic Algorithm III (U-NSGA-III) (Seada and Deb, 2016). The SWAT model simulates the PDMMs and their impacts on the basin hydrology. The U-NSGA-III identifies near-optimal allocations of PDMMs that minimise the severity of both agricultural and hydrological droughts. The methodology is tested in the Cesar River Basin (Colombia).

2. Study area

For a specific application of this framework, we choose the Cesar River Basin (17,369 km^2) as the study area. The basin's topography defines three distinct climatic regions: La Sierra Nevada de Santa Marta in the northwest (see red dots Fig. 1a), La Serranía del Perijá in the east (see blue dots Fig. 1a), and the Cesar River valley with the Zapatosa marsh from northeast to south (see grey dots Fig. 1a) (Universidad del Atlantico, 2014). La Sierra Nevada de Santa Marta comprises steeply sloped mountains reaching up to 5700 m above sea level (masl). In this sector, temperature ranges from 3 °C to 6 °C, and the mean annual precipitation is 1000 mm. Meanwhile, La Serranía del Perijá is an extension of the eastern branch of the Andes range in the east, having an elevation range from 1000 to 2000 masl. The average temperature is 24 °C, and the average annual precipitation varies from 1000 mm to 2000 mm. Lastly, the valley of the Cesar River up to the confluence with

the Zapatosa marsh is characterised by flat topography and a complex system of marshes formed by the Cesar River floodplains. The average temperature is 28 °C, and the mean annual precipitation is 1500 mm. Dominant crops in the Cesar River basin include oil palm, coffee, corn, and cassava. These four crops accumulate >70 % of the cultivated area in the basin and account for 90 % of the basin's agriculture GDP.

The Expansion of water-intensive crops, inappropriate cropping patterns, and lack of land suitability analysis for agriculture severely exacerbate water scarcity in the study area (Universidad del Atlantico, 2014). In La Sierra Nevada de Santa Marta and La Serranía del Perijá, deforestation driven by agricultural land expansion has impacted the discharge of the Cesar River's tributaries. <30 % of the primary forest remains in these areas (Agencia de Desarrollo Rural et al., 2019). In La Sierra and Serranía foothills, cattle raising and intensive agriculture have compromised soil structure, reducing infiltration rates (generally associated with high soil compaction). In a basin's drought situation assessment, Paez-Trujilo et al. (2023) showed that an unbalanced water cycle that favours water loss through evapotranspiration and limits percolation causes severe agricultural and hydrological drought conditions in the Cesar River valley and La Sierra and La Serranía foothills.

According to the Regional study of soil suitability for agriculture (2018), suitable land for agriculture is found in the middle part of the valley, the river floodplains, and in La Serranía del Perijá and La Sierra Nevada foothills. In practice, agricultural land allocation considerably differs from soil's suitability. Notably, the river valley is underused, and soils in the basin's northwest and La Serranía del Perijá foothills are overexploited, as shown in Fig. 1c (Agencia de Desarrollo Rural et al., 2019; Instituto Geografico Agustin Codazzi and Corporacion Autonoma Regional del Cesar, 2018).

3. Methodology

The proposed workflow consists of hydrological modelling, drought analysis and optimisation steps (see Fig. 2). Firstly, hydrological modelling is used to represent the basin hydrology, simulate the variables required to analyse droughts in the baseline scenario, i.e., soil moisture and streamflow, and parametrise the PDMMs. The baseline scenario represents the current drought situation and is the basis for comparing the effect of implementing PDMMs on droughts. Secondly, we apply the threshold level method (Yevjevich, 1967) to identify the drought events during the analysis period and estimate their severity levels. Thirdly, we develop and apply an optimisation engine to identify
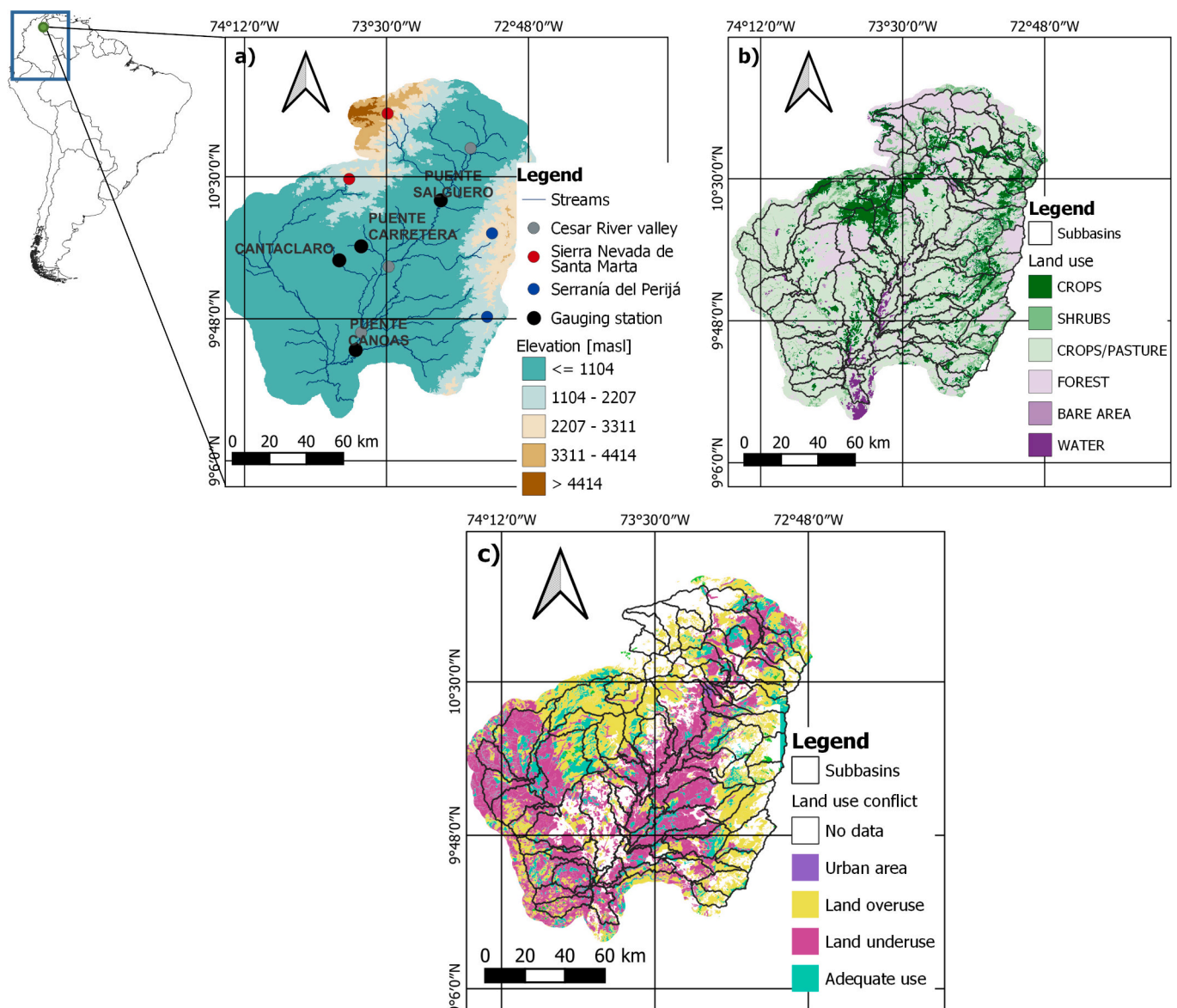

Fig. 1. Cesar River basin: a) topography, b) land use, and c) land use-conflict.

OPTIMISATION ENGINE

PDMMs
1. RWH ponds
2. Plantation crops allocation
3. Row crops allocation
4. Forest conservation
5. Channel protection
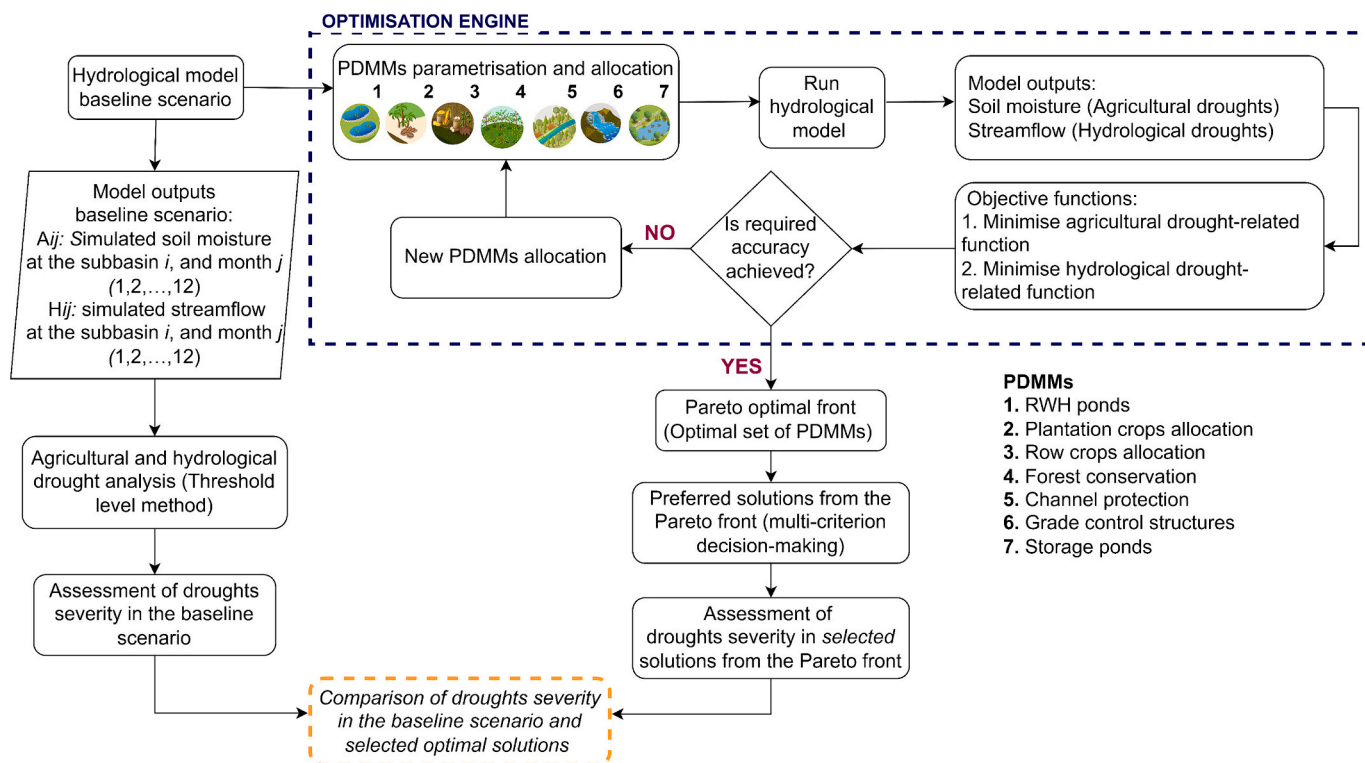**6.** Grade control structures
7. Storage ponds

Fig. 2. Flowchart of the methodology

the optimal sets of PDMMs that contribute to reducing the severity of droughts. To solve the optimisation problem in Python, we used the optimisation framework *pymoo* (Blank and Deb, 2020) coupled with a python wrapper for executing SWAT (i.e., *SWAT-pytools*; (Hernandez-Suarez and Nejadhashemi, 2022)). Once the optimisation is completed and the Pareto-optimal solution set is obtained, two multi-criterion decision-making (MCDM) methods are applied to select a few preferred solutions that balance the objective functions. Lastly, we compare the drought severity in the baseline scenario with the severity in the optimal solution for each objective function and the preferred solutions. A detailed description of the methodology is presented below.

3.1. Hydrological modelling

A SWAT model with an ArcSWAT extension was used to develop the hydrological model of the Cesar River basin. SWAT is a semi-distributed, continuous-time, process-based, watershed-scale model developed by The Agricultural Research Service of the United States Department of Agriculture (ARS-USDA). The model is intended to simulate surface and groundwater quantity and quality and to evaluate the long-term effects of land use and climate change on basin hydrology, sediment, and agricultural chemical yields (Neitsch et al., 2011). SWAT divides the basin area into subbasins up to the outlet point. Each subbasin is further split into Hydrological Response Units (HRUs), which are areas within the subbasin with common combinations of land cover, soil type and slope (Arnold et al., 2012).

The Cesar River basin model was built for the period from 1987 to 2018. The basin was divided into 108 subbasins with a median area of 160 km^2. Four slope classes were set for the HRUs generation: flat (0–2 %), gentle (2–10 %), steep (10–35 %) and considerably steep (>36 %). Table 1 presents the details and sources of the input data utilised for the model set-up. The following methods were used to simulate the main hydrological processes: the soil conservation service-curve number (SCS-CN) was used to represent surface runoff; potential evapotranspiration was estimated using the Hargreaves method; and water was

Table 1
SWAT model input data.

Data type	Details	Source
Digital elevation model	25 × 25 m	Dataset ALOS PALSAR L1.0, Cartography 1:25000 Geographic Institute Agustín Codazzi (IGAC), Colombia
Soil map	300 × 300 m	Soil profiles Project GEF Magdalena–Cauca VIVE, GEF, BID, Fundación Natura, Colombia
Land use map	25 × 25 m	Land use map Geographic Institute Agustin Codazzi (IGAC), Colombia
Daily precipitation and daily minimum and maximum temperature	Period 1985–2018 (34 years)	Institute of Hydrology, Meteorology and Environmental Studies (IDEAM), Colombia

routed through the channel network using the variable storage routing method.

3.1.1. Model calibration and validation

The model was calibrated using streamflow data from 1985 to 2002 and validated with data from 2003 to 2018, utilising records from four stream gauges (see black dots Fig. 1a). In both calibration and validation processes, the initial two years were designated as a warm-up period. Accordingly, performance indicators were computed for the periods 1987 to 2002 (calibration) and 2005 to 2018 (validation). The source of the streamflow data is the Institute of Hydrology, Meteorology and Environmental Studies (IDEAM), Colombia.

The model's performance for simulating streamflow was evaluated using the Nash-Sutcliffe Efficiency (NSE) and percent bias (PBIAS), represented by Eqs. (3) and (4). The NSE is a dimensionless indicator ranging from -∞ to 1, with 1 representing a perfect match between the observed and simulated values (Moriasi et al., 2007). The PBIAS measures the average tendency of the simulated values to be larger or smaller than the observed values. The ideal PBIAS is 0, with low-magnitude values indicating accurate model simulation (Moriasi et al.,

2007).

$$NSE = 1 - \frac{\sum\limits_{i=1}^{N} (O_i - P_i)^2}{\sum\limits_{i=1}^{N} (O_i - \overline{O})^2} \qquad (1)$$

$$PBIAS = \frac{\sum\limits_{i=1}^{N} (O_i - P_i) \times 100}{\sum\limits_{i=1}^{N} O_i} \qquad (2)$$

where O_i is the observed data, P_i the predicted data, $\overline{O}$ the mean of the observed data and N the number of observations during the simulation period.

Table 2 summarises the calibration and validation performance indicators for the SWAT model at each gauging station. The calibration and validation models simulated monthly stream flows with NSE values equal to or >0.50 and relatively low PBIAS values (GEF et al., 2020, 2021). According to the performance ratings for hydrological model calibration and validation, these NSE and PBIAS values indicate that the model is adecuate for simulating streamflow (Moriasi et al., 2007). Fig. 3 displays the model hydrographs at each gauging station for both the calibration and validation periods. A comprehensive description of the model setup, calibration, and validation procedure is presented in GEF et al. (2021,2020).

3.2. PDMMs selection and parametrization in SWAT

In this study, we selected seven interventions and practices to evaluate their effectiveness as PDMMs. Interventions were selected to cover the land and water phases of the hydrological cycle. Additional selection criteria included compatibility with the basin's land use and availability of parameters to represent the intervention in the SWAT model. The selected PDMMs, the parameters used to represent them in SWAT, and their values are summarized in Table 3. A description of each PDMM is provided below.

3.2.1. PDMM-1: infiltration ponds

Infiltration ponds are a Rainwater Harvesting technique (RWH) aiming to increase the soil water content in the soil profile by storing rain when it falls (Huang et al., 2021). This intervention contributes to increasing infiltration and groundwater recharge and decreases soil erosion by reducing surface runoff velocity (Nyagumbo et al., 2019; Piemontese et al., 2020). The Infiltration ponds were modelled in SWAT using the pothole routine (Wambura et al., 2018). Potholes are water bodies located off the main channel, and water flows to them from the subbasin (Du et al., 2005). The potholes were applied at the HRU level and represented by two parameters: the fraction of flow from the upland HRUs that contributed to the pothole HRU (POT_FR) and the maximum water depth inside the pothole (POT_VOLX). For the present study, the RWH pond's storage capacity was aggregated into one pothole, as there could be only one in each HRU.

The effect of an RWH pond on the overall water balance at each HRU is controlled by its storage capacity, which is given by the product between POT_FR times the HRU draining area and POT_VOLX (Neitsch

et al., 2011). Higher storage capacity generally results in higher evapotranspiration and soil water content, as well as lower surface runoff (Wambura et al., 2018). In our modelling approach, the infiltration pond's strength as a PDMM measure is defined by POT_FR given a fixed POT_VOLX. Higher POT_FR implies higher storage capacity, whereas POT_VOLX can be defined in terms of the average surface runoff depth aimed to be stored. In this study, POT_FR was set as 0.3 (i.e., an application level of 30 % at each HRU), whereas POT_VOLX was set as 20 cm, which represents infrastructure suitable to store approximately 35 % of the average surface runoff depth during the wet period in the study area.

3.2.2. PDMM-2 and PDMM-3: crops allocation

Allocating crops regarding climate, hydrology, terrain, and soil qualities maximises land production, prevents water scarcity, and reduces topsoil and groundwater depletion (Akpoti et al., 2019; Mosleh et al., 2017). Adequate crop allocation is crucial for maintaining sustainable production and reducing environmental impact (Bhat et al., 2023). In SWAT, the allocation of the main crops in the basin (oil palm coffee, corn and cassava) was simulated using the SCS runoff curve number for moisture condition II (CN2), the plant identification (PLANT_ID), the management operation number (MGT_OP) 1 for planting and 5 for harvest and kill, and the month and day in which the operation takes place (MONTH/DAY). The CN2 value was assigned for each hydrologic soil-cover complex (combination of hydrological soil group and land use) according to SWAT's crop database. It is worth noting that CN2 is the main parameter controlling the strength of a specific crop as a PDMM measure. Higher CN2 values indicate lower infiltration capacity and higher runoff potential from a particular area. Meanwhile, the MONTH/DAY of planting, harvest and kill operations of each crop were set conforming to the National Agricultural Survey (DANE, 2019).

3.2.3. PDMM-4: Woodlands' allocation

Forest conservation/restoration includes forest regeneration, species diversity, and unevenly aged stands. This intervention contributes to limiting soil degradation to slow runoff and increase infiltration and groundwater recharge. In this study, the CN2 value for forested areas in good hydrological conditions represented the intervention. Similarly to the previous sets of PDMMs, CN2 is the model parameter defining the strength of this measure. Depending on the hydrologic soil group, woodlands are generally associated with CN values ranging from 30 to 80 (Neitsch et al., 2011). The CN2 value was assigned for each hydrologic soil-cover complex according to SWAT's crop database. In practice, the selected values to model this intervention represent forests with diverse tree species, the presence of native species, and adequate soil structure and water balance. Overall, forests in these conditions are protected areas dedicated to forest conservation.

3.2.4. PDMM-5 and PDMM-6: channel restoration: channel protection and grade control

Channels restoration refers to changes in the physical structure of a river channel, its riparian zone or the floodplain through reshaping, reconstruction, or replanting (Muhar et al., 2018; Wohl et al., 2015). These modifications aim to amend hydrologic, geomorphic, and/or ecological processes within degraded or altered water bodies. Over the last few years, river restoration has shifted to a process-based restoration approach considering rivers' geomorphology and function (Greene et al., 2023; Wohl et al., 2015). There is a comprehensive list of interventions used for channel restoration, e.g., reconfiguration of stream channels, floodplain reconnection, and riparian revegetation (Ciotti et al., 2021; Inamdar et al., 2023). In this study, we focus on the bank and bed channel protection and grade control.

Channel protection controls the river's bank degradation, balances the sediment load, and reduces water velocity adjacent to the streambank (Li and Eddleman, 2002; Pinto et al., 2016; Rosgen, 2001). In this

Table 2
SWAT model performance simulating streamflow.

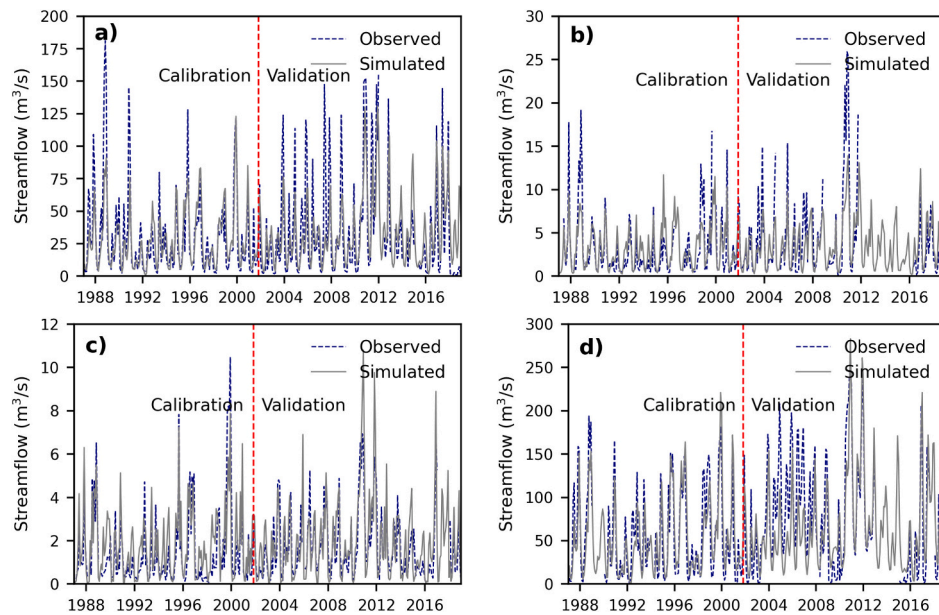| Gauging station	Calibration		Validation	
	NSE	PBIAS [%]	NSE	PBIAS [%]
Puente Salguero	0.61	4.28	0.52	−8.3
Puente Carretera	0.50	−5.34	0.52	7.6
Cantaclaro	0.58	−11.30	0.50	−11.7
Puente Canoas	0.70	−1.34	0.57	10.64

Fig. 3. Monthly calibration and validation for streamflow at: a) Puente Salguero, b) Puente Carretera, c) Cantaclaro and d) Puente Canoas; Fig. 1a presents the location of the gauging stations. From Multivariate regression trees as an "explainable machine learning" approach to explore relationships between hydroclimatic characteristics and agricultural and hydrological drought severity: case of study Cesar River basin by Paez-Trujillo et al., 2023, Natural Hazards and Earth System Sciences 23, 3863–3883.

study, channel protection was modelled using SWAT model parameters such as Manning's "n" value for the main channel (CH_N(2)) and the channel cover factor (CH_COV2). Grade stabilization refers to any intervention that provides stability to the streambed. These interventions range from loose rock structures (e.g., steep-pool sequence) to reinforced concrete weirs, and they vary in scale from small to large rivers (Wang et al., 2017). Controlling channel degradation prevents failures of the channel banks by over-heightening and preventing potential groundwater table lowering caused by channel widening and bank erosion (Natural Resources Conservation Service, 2007). Here, channel protection was modelled using SWAT parameters such as the average slope of the main channel along the channel length (CH_S(2)) and the channel cover factor (CH_COV2). Overall, increases in CH_N(2) due to the introduction of large and rough bed materials and dense vegetation, and reductions in CH_S(2) result in lower stream velocities, which favour aggradation processes and greater residence times within the river network. Meanwhile, fully protected channels (i.e., CH_COV2 equal to zero) normally result in lower sediment yields from channel erosion. In the field, the values used to simulate channel protection can be associated with works such as riverbank riprap, retaining walls and bioengineering (e.g., pole plantings or coir rolls). In turn, grade stabilization values represent, for instance, treated wood structures or cattle panel structures. In general, applying these strategies requires thorough hydrogeomorphic studies to determine the most adequate structure and can be costly.

3.2.5. PDMM-7: storage ponds

Check dams, small barriers constructed across channels or gullies, serve the purpose of impeding the flow. These structures store flood-water, increase the basin's retention capacity and allow more time for water percolation to recharge aquifers, among other functions (Abbasi et al., 2019; Lucas-Borja et al., 2021; Wang et al., 2021). In the SWAT model, we simulated check dams as ponds (Waidler et al., 2009). SWAT defines ponds as water bodies within the subbasin area, exclusively receiving loadings from the subbasin's HRUs. The model allows the allocation of only one pond at each subbasin; then, the predicted runoff from the HRUs is aggregated and routed into the pond situated at each subbasin (Jalowska and Yuan, 2019; Rabelo et al., 2021). SWAT model

parameters employed to represent the intervention are the fraction of the subbasin that drains into ponds (POND_FR), the surface area of ponds when filled to the principal spillway (POND_PSA), and the volume of water stored in ponds when filled to the principal spillway (POND_PVOL). Like infiltration ponds, water storage is determined by POND_FR, given POND_PSA and POND_PVOL values which are check dams' design parameters. Therefore, the storage pond's strength as a PDMM measure is defined mainly by POND_FR.
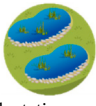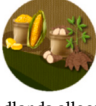
3.3. Agricultural and hydrological drought analysis

Drought analysis was conducted using the threshold level method. This approach is suitable for quantifying the water required to manage and recover from a drought (Iglesias et al., 2018). According to the threshold level method, a drought is a period (days, weeks, or months) during which a variable of interest (e.g., precipitation, soil moisture, or streamflow) remains below a predetermined threshold (τ) (Tallaksen et al., 2009; Yevjevich, 1967; Zelenhasić and Salvai, 1987). Generally, the threshold lies between the variable distribution's fifth and thirtieth percentiles (Herrera-Estrada et al., 2017; Heudorfer and Stahl, 2017; Hisdal et al., 2024). Each drought event can be characterised by its duration, spatial extent, and severity, among other characteristics (Hisdal et al., 2024; Zhang et al., 2022). In this study, simulated soil moisture and streamflow are the variables used to represent agricultural and hydrological droughts, whereas severity is the feature of interest. Drought severity was estimated separately for the baseline or current scenario (represented by the calibrated models of the Cesar River basin) and the management scenarios (selected most-preferred trade-off solutions from the Pareto front) obtained from the optimisation.

3.3.1. Setting the drought thresholds

This study uses the SWAT model outputs, namely, soil moisture and streamflow, to calculate agricultural and hydrological drought thresholds, respectively. SWAT results obtained at the subbasin level allow us to estimate the drought severity at each subbasin and assess the differential effect of the mitigation measures in upstream and downstream subbasins.

The simulated soil moisture $A_i(t)$ at the subbasin i $(1, 2, …, N)$ in the

Table 3
PDMM applied to reduce the severity of agricultural and hydrological droughts.

ID	Preventive drought management measures (PDMM)	Parameter(s) used in SWAT	Value when PDMM is applied in a HRU or subbasin
PDMM-1	RWH ponds	POT_FR [a] (.hru), POT_VOLX [b] (.hru).	0.3 20 [cm]
PDMM-2	Plantation crops allocation (e.g., oil palm or coffee)	CN2 [c] (.mgt) MGT_OP MONTH/DAY	45, 66, 77 or 80 1 1/1
PDMM-3	Row crops allocation (e.g., corn or cassava)	CN2 [c] (.mgt) PLANT_ID MGT_OP MONTH/DAY MGT_OP MONTH/DAY	67, 77, 83 or 87 CORN 1 3/1 (main harvest) 7/1 (second harvest) 5 8/1 (main harvest) 11/1 (second harvest)
PDMM-4	Woodlands allocation	CN2 [c] (.mgt)	25, 55, 70 or 77
PDMM-5	Channel protection	CH_N2 [d] (.rch), CH_COV2 [e] (.rch)	CH_N2 reduced 0.15 from the default value. 0.0 (fully protected river channel)
PDMM-6	Grade control	CH_S(2) [f] (.rch), CH_COV2 [e] (.rch)	Reduced by 10 % from the default value. 0.0 (fully protected river channel)
PDMM-7	Storage ponds	POND_FR [g] (.pnd), POND_PSA [h] (.pnd), POND_PVOL [i] (pnd)	0.3 20 [Ha] 1.5 [10^4 m^3]

[a] Fraction of the HRU area that drains into a pothole.
[b] Maximum volume of water stored in the pothole over the entire HRU (mm).
[c] Initial SCS runoff curve number for moisture condition II.
[d] Manning's "n" value for the main channel.
[e] Channel cover factor.
[f] Average slope of main channel along the channel length (m/m).
[g] Fraction of subbasin area that drains into ponds.
[h] Surface area of ponds when filled to principal spillway (ha).
[i] Volume of water stored in ponds when filled to the principal spillway (10^4 m^3 H$_2$O).

baseline scenario is used to set the monthly agricultural threshold τ_{ij}^A, where $j\,(1, 2, ..., 12)$. The monthly threshold at each subbasin corresponds to the 20th percentile of the empirical distribution function of the series $\left(A_{ij1}, A_{ij2}, ...A_{ijn}\right)$, where n is the simulation year. Similarly, the simulated streamflow $H_i(t)$ at the subbasin $i\,(1, 2, ..., N)$ in the baseline scenario is used to set the monthly hydrological threshold τ_{ij}^H, where $j\,(1, 2, ..., 12)$. The monthly threshold at each subbasin corresponds to the 20th percentile of the empirical distribution function of the series $\left(H_{ij1}, H_{ij2}, ...H_{ijn}\right)$, where n is the simulation year.

3.3.2. Identifying drought events and estimating the drought severity

We identified the agricultural and hydrological drought events during the period of analysis employing the monthly thresholds. In this study, the agricultural drought state is assumed to occur in a subbasin when the monthly simulated soil moisture $A_i(t)$ remains below the set threshold $\left(A_i(t) < \tau_{ij}^A\right)$. Likewise, the hydrological drought state is assumed to occur in a subbasin when the monthly simulated streamflow $H_i(t)$ falls below the set threshold $\left(H_i(t) < \tau_{ij}^H\right)$.

To consider a drought state in a subbasin part of a drought event, a temporal and spatial conditions were set. A drought (agricultural or hydrological) is assumed to occur in the basin when a number of subbasins (covering at least 30 % of the basin's total area) are in a drought state for at least two consecutive time steps (i.e., in this study we used one month as the time step). A drought begins when both conditions are satisfied and lasts until one of the conditions is not satisfied. It is worth highlighting that the minimal extension of a drought is not defined, but it is acknowledged that droughts usually occur on a wide scale (Sheffield and Wood, 2011). Setting a spatial threshold is a common practice to keep a minimum drought-affected area and avoid identifying isolated regions experiencing dry spells as drought events (Brunner et al., 2021).

After identifying the drought events in the analysis period, the agricultural and hydrological drought severity (deviation from the threshold) is estimated at each subbasin (Eqs. (3), (4)).

$$S_i^A(t) = \begin{cases} \tau_{ij}^A - A_i(t) \text{ if } A_i(t) < \tau_{ij}^A \\ 0 \text{ if } A_i(t) \geq \tau_{ij}^A \end{cases} \tag{3}$$

$$S_i^H(t) = \begin{cases} \tau_{ij}^H - H_i(t) \text{ if } H_i(t) < \tau_{ij}^H \\ 0 \text{ if } H_i(t) \geq \tau_{ij}^H \end{cases} \tag{4}$$

where $S_i^A(t)$ represents the agricultural drought severity at the subbasin i at time step t (in mm), and $S_i^H(t)$ represents the hydrological drought severity at the subbasin i at time step t (in mm d^{-1}). Note that the severities here (Eqs. (3) and (4)) are defined as deviations from the threshold without normalization. Thus, $S_i^A(t)$ takes the same unit as soil moisture (here in mm) and $S_i^H(t)$ takes the same unit as streamflow (here in mm d). Higher the negative values of the severities, more severe are the droughts.

3.3.3. Comparison of drought severity between the baseline scenario and the selected solutions from the Pareto front

The drought severity change was evaluated by comparing the severity in the baseline scenario to the severity in the near to-optimal drought management scenarios obtained from the optimisation. Eqs. (5) and (6) were employed for this purpose.

$$\Delta S_i^A(t) = \frac{S_i^A(t)_{BL} - S_i^A(t)_{OP}}{S_i^A(t)_{BL}} \times 100 \tag{5}$$

$$\Delta S_i^H(t) = \frac{S_i^H(t)_{BL} - S_i^H(t)_{OP}}{S_i^H(t)_{BL}} \times 100 \tag{6}$$

where $\Delta S_i^A(t)$ is the change in agricultural drought severity (%) at the subbasin i at time step t; $\Delta S_i^H(t)$ is the change in hydrological drought severity (%) at the subbasin i at time step t; *BL* is the baseline scenario; and *OP* are the management scenarios obtained from the optimisation (selected most-preferred trade-off solutions from the pareto front). A positive change reflects a reduction in the severity of the drought relative to the baseline scenario, and a negative value shows an increase in the severity of the drought.

3.4. Formulation of the optimisation framework for PDMM planning

The optimisation process starts by initialising a population of drought management scenarios (diverse allocations of the PDMMs evaluated). For each drought management scenario, the measures and their potential allocations are put into SWAT to simulate the PDMMs' impact on the basin hydrology, particularly on soil moisture and streamflow. Then, agricultural and hydrological drought objectives are computed using the hydrological modelling outcomes. U-NSGA-III is applied to obtain near-optimal solutions, minimising both agricultural and hydrological drought objectives. Thus, the outcome of the optimisation process is a Pareto front containing a set of solutions (management scenarios with different PDMMs combinations and allocations) that contribute to reducing the severity of agricultural and hydrological droughts. To solve the optimisation problem in Python, we used the optimisation framework *pymoo* (Blank and Deb, 2020) coupled with *SWAT-pytools*, which includes a wrapper for modifying SWAT input files. The optimisation runs were executed in the Snellius supercomputer (Dutch National Supercomputer Snellius, 2023). In Snellius, the compute nodes are grouped into partitions; we ran the optimisation in the Genoa partition, which includes 128 cores per node and the memory per node is 336 GiB. To run the simulation, the number of CPUs per task was one and the requested memory per CPU was 3GB. Below, we describe the formulation of the problem of allocating PDMMs as an optimisation problem.

3.4.1. Objective functions

Two competing objective functions were formulated to identify the optimal PDMMs sets that reduce the severity of agricultural and hydrological droughts. The first objective is based on minimisation of the agricultural drought severity (Eq. (7)). The Objective Function 1 (OF1) was formulated as the aggregation (over the simulation period) of the difference between the average available water capacity (AWC) of the soil and the simulated soil moisture at each subbasin during the dry season months (Dec, Jan, Feb, Mar, Apr, May, Jun, Jul). AWC refers to the soil's ability to store and provide water to plant roots and depends on the soil properties, particularly soil texture (Rabot et al., 2017). Further information on typical AWC values for different soil textures can be found at de Jong van Lier et al. (2023). Minimising the difference between AWC and the simulated soil moisture is intended to maintain an adequate water content in the soil profile (informed by the dominant soil texture at each subbasin) and prevent this value from falling below the agricultural drought threshold. We focused on dry months to force the optimisation engine to select drought management scenarios that contribute to reducing the soil water deficit during the dry season when droughts are more likely to occur and their severity tends to increase.

$$Min \sum_{i=1}^{m} \sum_{j=1}^{n} \left| AWC_{ST} - SW_{ij} \right| \tag{7}$$

where, $i = 1, 2, 3 \ldots n$ are the subbasins, $j = 1, 2, 3 \ldots m$ are the dry months over the years of the simulation period, AWC_{ST} is the average available water capacity of the dominant soil texture at the ith subbasin (in mm) and SW_{ij} is the soil moisture during the jth dry month at the ith subbasin (in mm).

The Objective Function 2 (OF2) (Eq. (8)) deals with hydrological drought and was formulated as the aggregation of the simulated streamflow at the outlet of each subbasin. Maximising the discharge aimed to increase the streamflow and prevent this value from falling below the hydrological drought threshold. The optimisation framework *pymoo* minimises all the objective functions. If an objective function is maximised (*max*f$_i$), the objective function can be formulated to minimise its negative value (*min* $-$ f$_i$) (Blank and Deb, 2020).

$$Min - \sum_{i=1}^{m} \sum_{j=1}^{n} q_{ij} \tag{8}$$

where, $i = 1, 2, 3 \ldots n$ are the subbasins, $j = 1, 2, 3 \ldots m$ are the months over the years of the simulation period, and q_{ij} is the discharge during the jth month at the outlet of the ith subbasin (in mm d^{-1}).

3.4.2. Decision variables

Fig. 4 shows a schematic of the decision variable matrix for planning drought mitigation measures. In this study, each matrix row (decision variable vector) represented a member of the population that consisted of genes defining a specific combination of PDMMs, or what is referred to as an allele. Each gene can have either a one or zero state, one indicating the measure is applied in a specific spatial unit (HRU or subbasin) and zero indicating the measure is not applied in that spatial unit. When the state is "one" in a spatial unit, all the parameters representing the measure are modified according to the values presented in Table 1. The number of alleles in a gene was given by the number of PDMMs applicable at each spatial unit. Four out of the seven evaluated PDMMs were applied at the HRU level (infiltration ponds, crop allocation, forest restoration), and the other three PDMMs were applied at the subbasin level (channel protection, grade stabilization and storage ponds). Accordingly, the number of alleles in an HRU gene was four and in a subbasin gene was three.

Considering the significant number of spatial units in the basin model, the most susceptible spatial units to agricultural and hydrological droughts were selected for the optimisation process, that is to say, 855 out of 2699 HRUs and 78 out of 108 subbasins. Then, the number of decision variables (length of the decision variables vector) was given by the equation $N = (No_{HRU} \times 4) + (No_{sub} \times 3)$, where No_{HRU} is the number of HRUs selected to apply the PDMMs and No_{sub} is the number of subbasins selected to apply the PDMMs. The number of decision variables for the optimisation of PDMM in the Cesar River model was 3654, and the size of the matrix X was 3654 multiplied by the population size; in this study, 350 individuals.

To narrow down the decision variable space, the most susceptible subbasins to agricultural and hydrological droughts were selected using the study outcomes by Paez-Trujillo et al. (2023). Based on their results, we identified that subbasins located in the upper and middle part of the river valley are drought-prone areas, and multiple hydroclimatic factors influence their susceptibility to agricultural and hydrological droughts.

3.4.3. Optimization algorithm and convergence to near-optimal Pareto front

We used U-NSGA-III to identify strategic portfolios of PDMMs minimising hydrological and agricultural drought severity in the study area. U-NSGA-III is an algorithm developed to solve constrained and unconstrained optimization problems with one to more than three objective functions (Seada and Deb, 2016). As part of the NSGA-III family of algorithms, U-NSGA-III is an elitist population-based method that uses non-domination sorting, evolutionary operators such as crossover and mutation, and reference directions to find near-optimal Pareto solutions. Compared to the original NSGA-III version, U-NSGA-III introduces a niching-based selection procedure with no extra parameters to allow a seamless degeneration to mono- and bi-objective problems (Seada and Deb, 2016). Using the unified version of NSGA-III is intended to maintain consistency among solutions when increasing or reducing the number of objective functions and working with the same decision variables. In this study, we implemented U-NSGA-III using the *pymoo* library in Python 3.7 (Blank and Deb, 2020). Algorithm parameters include the number of reference directions (which equals the population size), the maximum number of generations (which operates as the stopping criterion), crossover and mutation probabilities, and the distribution indices for simulated binary crossover (SBX) and polynomial mutation. We generated well-spaced reference directions using the Riesz
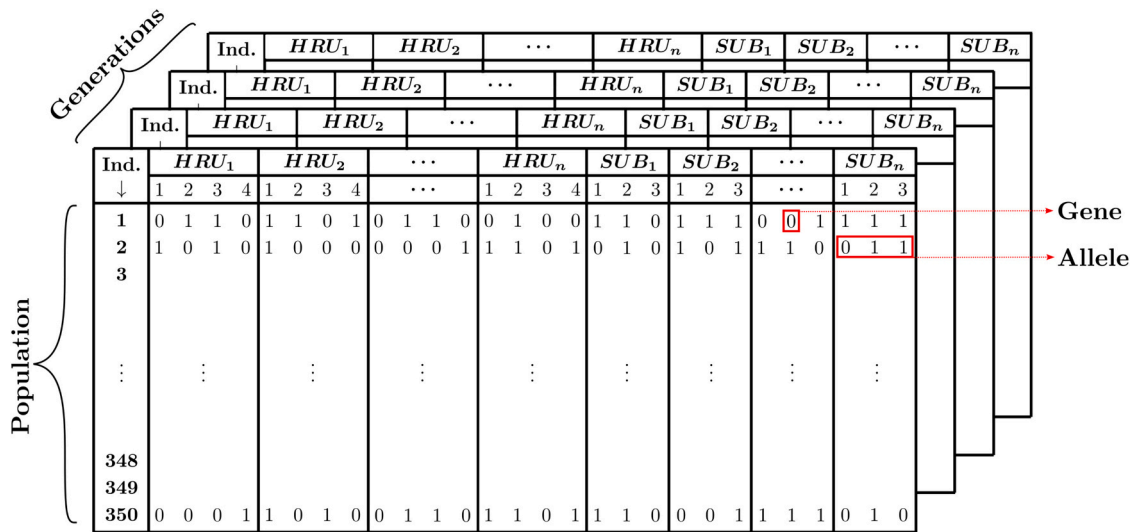
Fig. 4. Schematic of a decision variable matrix for planning drought mitigation measures.

s-Energy method (Blank et al., 2021). Table 4 presents the parameter values used in this study, which are standard and recommended.

On the other hand, we computed the Hypervolume Indicator at the end of each generation to evaluate convergence to a near-optimal Pareto solution. The hypervolume represents the region collectively dominated by a set of Pareto solutions in the objective space (Auger et al., 2012). Therefore, the Hypervolume Indicator is usually employed for convergence assessment since it simultaneously accounts for the proximity of the points to the actual Pareto front, diversity, and spread. Since a larger hypervolume occurs when the Pareto solutions are closer to the origin of the objective space, a higher Hypervolume Indicator is considered better in minimization problems. Moreover, if the Hypervolume Indicator shows a near-steady behaviour with increasing generations, it indicates that the Pareto front has stabilized and that convergence has eventually occurred (Raschke et al., 2021).

3.4.4. Preferred trade-off solutions

Once we obtained the near-optimal Pareto set, we selected a few preferred solutions balancing the objective functions using two different multi-criterion decision-making (MCDM) approaches. In the first approach, we computed a pseudo-weight vector for each solution in the Pareto set (Deb, 2001). In this vector, the *i*-th element represents the relative importance of the *i*-th objective function for a particular solution and is computed using Eq. (9).

$$w_i = \frac{\left(f_i^{max} - f_i\right) \Big/ \left(f_i^{max} - f_i^{min}\right)}{\sum_{m=1}^{M}\left(f_m^{max} - f_m\right)\Big/\left(f_m^{max} - f_m^{min}\right)} \tag{9}$$

where f_i^{min} and f_i^{max} are the minimum and maximum values of the *i*-th objective function, respectively. It is worth noting that when computing the pseudo-weight vector, the sum of all elements is forced to one. This study identified the most balanced solution with a pseudo-weight close to (0.5, 0.5). Two additional preferred solutions were obtained using

additional target vectors, (0.25, 0.75) and (0.75, 0.25), to indicate a preference for one of the objective functions. In the second approach, we identified knee points in the Pareto set, which are solutions showing high trade-offs. These points result in a slight gain in one objective while having a high loss in the other when moving along neighbouring solutions. Defining whether a trade-off is high or low requires the definition of a threshold, which in this study was taken as the average trade-off plus twice the standard deviation using the entire Pareto set. We implemented the high trade-off procedure proposed by Rachmawati and Srinivasan (2009), included in *pymoo*, to identify any knee points. Then, we selected the knee point with the most balanced pseudo-weight vector as a preferred solution.

4. Results

4.1. Drought events in the baseline scenario

We identified the drought events in the analysis period by applying the method described in 3.3. The date and duration of the identified droughts were consistent with the agricultural and hydrological drought events found by Paez-Trujillo et al. (2023) using the Soil moisture deficit index (SMDI) and the Standardized Streamflow Index (SSI). Furthermore, drought events agreed with the chronology of drought events in Colombia described at the National Study of Water (Instituto de hidrología meteorología y estudios ambientales (IDEAM), 2019). Table 5 shows the dates and duration of the drought events. Fig. 5a and b show

Table 4
U-NSGA-III parameters and their values for this study.

Parameter	Value
Number of reference directions (population size)	350
Max. number of generations	350
Crossover probability	0.9
Mutation probability	1/3654
Distribution index – SBX (Crossover)	10
Distribution index – Polynomial mutation	20

Table 5
Agricultural and hydrological droughts during the period of analysis.

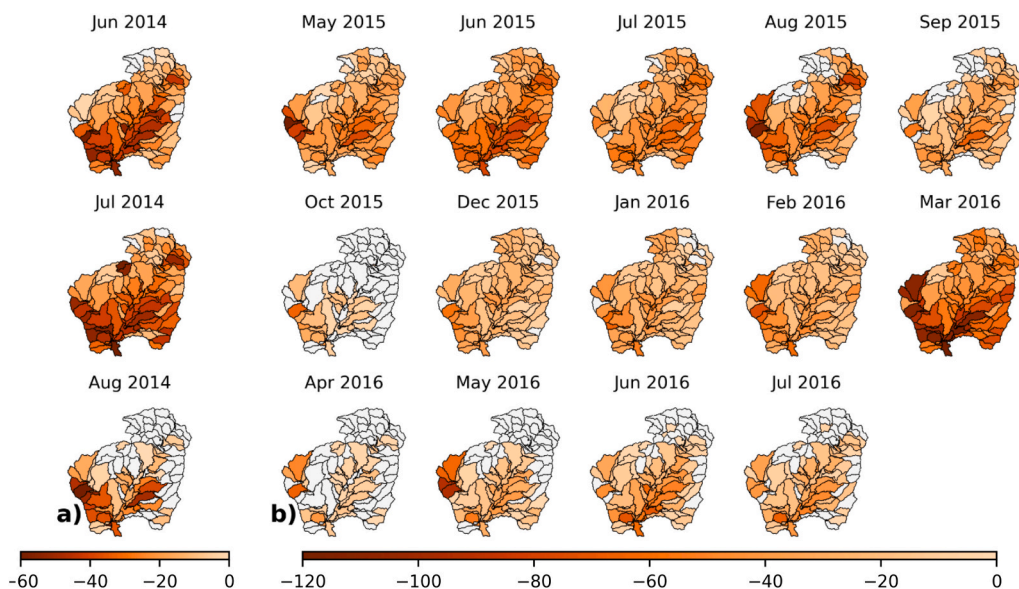| Event	Agricultural droughts		Hydrological droughts	
	Date	Duration [months]	Date	Duration [months]
I	May 1991 – Jun 1992	13	Apr 1991 – May 1992	14
II	Jun 1997 – April 1998	11	Apr 1997 – Feb 1998	11
III	Jun 2001 – Aug 2001	3	May 2001 – Jun 2001	2
IV	Oct 2009 – Jan 2010	4	Sep 2009 – Nov 2009	3
V	Jun 2014 – Aug 2014	3	Jun 2014 – Jul 2014	2
VI	May 2015 – Jul 2016	14	Apr 2015 – Apr 2016	13

Fig. 5. Agricultural drought severity events a) V and b) VI in mm.

the monthly drought severity of the agricultural drought events V and VI, and Fig. 6a and b show the monthly drought severity of the hydrological drought events V and VI. These two events were the most severe droughts observed in the analysis period and were selected to assess the effect of PDMM on the severity of short-term and long-term droughts.

Overall, the drought severity of the drought events evaluated varied in time and space. For agriculture droughts, the highest deficit was observed in the basin west, in the river valley, and upstream of the basin outlet (Fig. 5a and b). During the short-term event, agricultural severity was alike in the first two months, and in the last month, the area in drought condition and the severity reduced (Fig. 5a). In the long-term event, severity slightly increased for the first five months. In October and November, there was a recovery period. Then, in December, the severity increased until March (Fig. 5b). Regarding hydrological droughts, the highest deficit occurred in the mountainous areas in La Sierra and La Serranía. During the short-term event, the drought severity

did not vary markedly (Fig. 6a), and in the long-term event, the highest deficits were observed in May, June, September and October (Fig. 6b).

4.2. Pareto optimal front and allocation of the PDMMs for the most-preferred trade-off solutions

Fig. 7 shows that U-NSGA-III progressed towards a near-optimal Pareto front, considering the stable behaviour of the Hypervolume indicator at the end of the optimisation run.

A relatively uniform distribution of the objective vectors in the front is presented in Fig. 8. The initial population consisting of 350 randomly generated individuals evolved into a well-spread and evenly distributed convex Pareto front. The final Pareto front consisted of 258 optimal solutions and was obtained after 350 generations (i.e., 122,500 function evaluations). Once the optimisation was completed, we selected six solutions from the Pareto-optimal front (Fig. 8. points *a* to *f*) to analyse the

Fig. 6. Hydrological drought severity events a) V and b) VI in mmd^{-1}.

Fig. 7. Hypervolume indicator at the end of each U-NSGA-III generation.

Fig. 8. Optimal Pareto front obtained from the 350th generation and most-preferred trade-off solutions for the PDMM allocation problem. Each point represents a set of PDMMs to be allocated (points *a* to *f*). The solution of the baseline scenario (blue dot) is also shown for reference.

spatial distribution of the seven PDMMs evaluated (see Table 3) and compare the droughts' severity in the baseline scenario with the severity in the selected solutions. The MCDM approaches utilised to select the solutions *b, c, d* and *e* are described in 3.4.4.

4.3. Optimal allocation of the PDMMs for the most-preferred trade-off solutions

Once the optimisation was completed, we selected six solutions from the Pareto-optimal front (Fig. 8. points *a* to *f*) to analyse the spat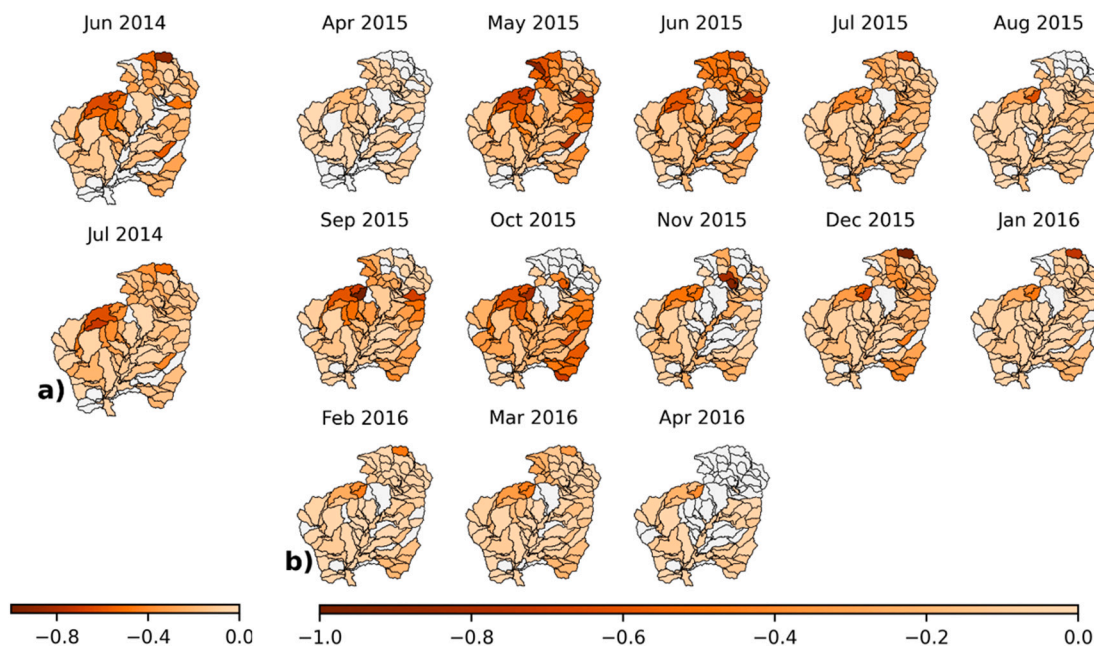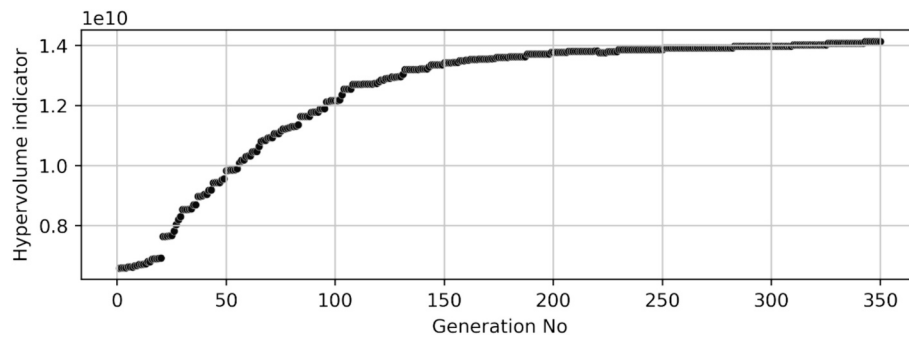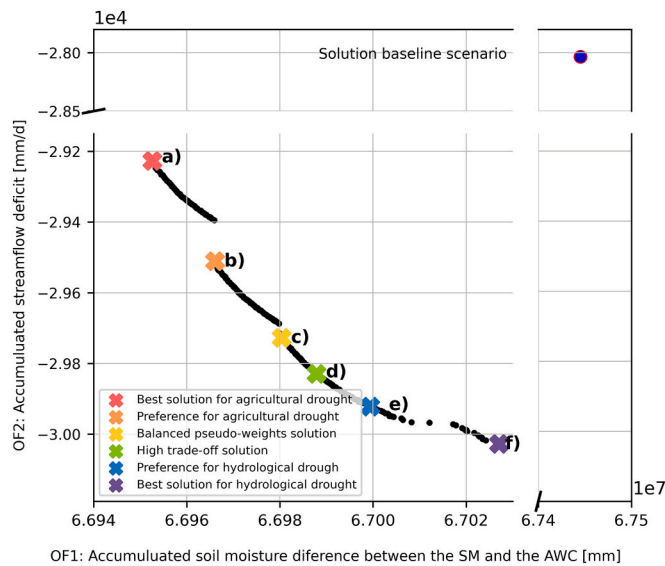ial distribution of the seven PDMMs evaluated (see Table 3) and compare the droughts' severity in the baseline scenario with the severity in the selected solutions. Fig. 9 presents the PDMMs allocation in the optimal solutions for agricultural (Fig. 9a) and hydrological (Fig. 9f) droughts, the selected most-preferred trade-off solutions, obtained through pseudo-weight and high trade-off methods (Fig. 9c and d) and the preferred trade-off solutions with preference for agricultural and hydrological droughts, selected through the pseudo-weight method (Fig. 9b and e). The MCDM approaches utilised to select the solutions *b, c, d* and *e* are described in 3.4.4.

Fig. 9a and b (PDMM-1) show that in scenarios with preference for agricultural drought management, RWH ponds were allocated in the river valley and in a strip that extends from the basin's north-east towards the west and in some subbasins at the basin's west and south. In

the scenarios with preference for hydrological drought management, RWH ponds were applied to a lesser extent (Fig. 9e and f, PDMM-1). RWH ponds were allocated in the northeast strip, especially at elevations >1000 m and in the mountainous areas in the basin's west. RWH ponds allocated at the river valley considerably decreased compared with scenarios with a preference for agricultural droughts.

RWH ponds allocation in the different solutions concurs well with previous studies concluding that suitable sites for RWH ponds depend on the intended application. For increasing soil moisture areas with low runoff potential given by precipitation ranging between 100 mm/year and <1000 mm/year, sandy soils and moderate slopes are recommended (Kahinda et al., 2008; Terêncio et al., 2017). Factors such as altitude, topography, and lithology are also evaluated to allocate RWH for groundwater recharge (Pacheco and Van Der Weijden, 2014).

In the solutions with preference for agricultural drought management, plantation crops (e.g., oil palm, coffee) were concentrated in the middle course of the river valley, and crop patches were observed in the headwater and the basin's south (Fig. 9a and b PDMM-2). Overall, crop allocation obtained from the optimisation process in solutions *a* and *b* agrees with the Regional study of soil suitability for agriculture (2018). In the best-trade-off solutions and solutions with preference for hydrological droughts, plantation crops were allocated in mountainous areas at relatively high altitudes (replacing woodlands), the basin's west and southeast (Fig. 9e and f PDMM-2). Earlier studies demonstrate that runoff, baseflow, and streamflow generation in oil palm plantations vary due to previous land cover, soil, and topographic conditions, showing a general increase compared to forest cover (Gómez et al., 2023). Nevertheless, other studies conclude that streamflow tends to decrease during low-flow months in land areas converted to oil palm (Heidari et al., 2020). In light of contrasting evidence, careful attention should be paid to crop allocation.

In the solutions with preference for agricultural drought management, the allocation of row crops was limited (Fig. 9a and b PDMM-3). These crops were allocated in scattered strips in the river valley and towards the basin's south. On the contrary, in solutions *e* and *f,* the allocation of row crops notably increased throughout the basin (Fig. 9e and f PDMM-3), including areas at relatively high altitudes. The allocation of corn in solutions *e* and *f* seems connected to the runoff potential of the curve number representing these crops. Curve number values to represent these crops are significantly high; then, it is expected that runoff contribution to the streamflow increases in the wet season, favouring the maximisation of the streamflow (OF2).

For solutions with preference for agricultural drought, forests in good hydrological condition spread over the basin area (Fig. 9a and b PDMM-4). Woodlands were allocated in the downhills of la Sierra Nevada, La Serranía del Perijá, the middle part of the river valley and in the basin's west. Woodlands were allocated in the Sierra and the Serranía del Perijá at relatively high altitudes for solutions with preference for hydrological drought management. Overall, woodland allocation is consistent with the Regional study of soil suitability for agriculture (2018). The study indicates that a thin topsoil and drainage density
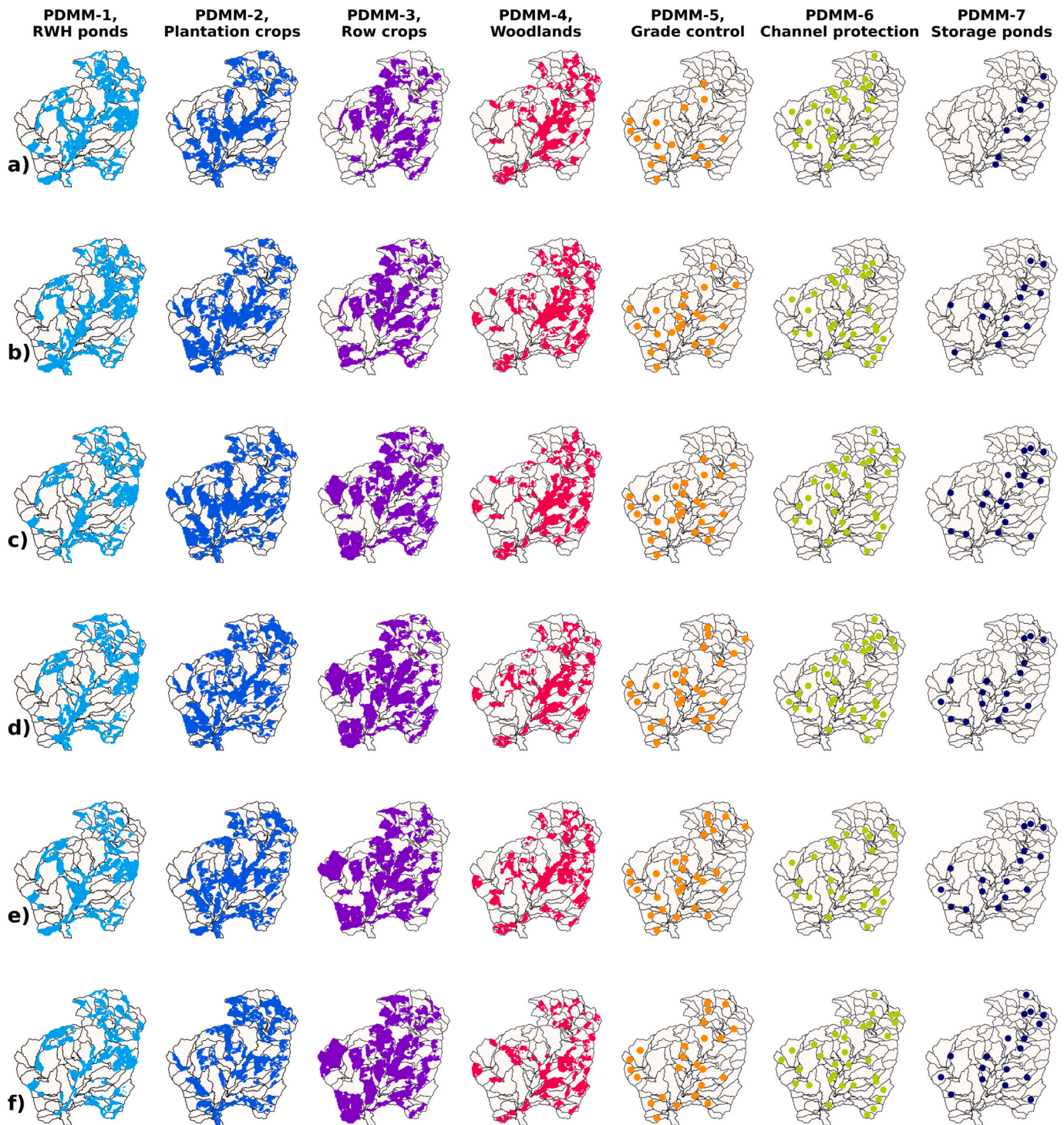
Fig. 9. Allocation of the PDDMs in the six selected Pareto-optimal solutions: (a) best solution for agricultural drought management, (b) trade-off solution with preference for agricultural droughts, (c) most-preferred trade-off solution selecting the most balanced pseudo-weight, (d) most balanced high trade-off solution, (e) trade-off solution with preference for hydrological droughts, and (f) best solution for hydrological drought management.

limits soil fertility in mountainous areas at elevations >2000 m. Hence, the land is suitable for forest conservation or restoration. Additionally, the allocation of woodlands in management scenarios aligns with findings in the literature indicating that planting native trees and fostering natural regeneration have regulated the annual streamflow and base flow since the first phases of restoration (Jones et al., 2022).

Channel protection structures are allocated towards the basin's west and in the middle part of the river valley in solutions giving more weight to agricultural droughts (Fig. 9a and b PDMM-5). It should be pointed

out that the SWAT model parameters used to represent this intervention do not influence the soil water content simulation; consequently, it has no impact on the severity of agricultural droughts. Considering this, in solutions *a* and *b*, the number of channel protection structures is low, mainly in the basin's west. In solutions giving more weight to hydrological droughts, channel protection allocates in the basin's west and the river valley from the headwater to the basin outlet.

Similarly, to channel protection structures, SWAT model parameters used to represent grade stabilization structures do not influence soil

water content simulation. In solutions, *a* and *b,* stabilization structures are observed towards the basin's west and the river valley (Fig. 9a and b PDMM-6). Most of these subbasins experienced the highest streamflow deficit during the drought events evaluated (Fig. 6a and b). The number of grade stabilization structures increases in solutions with preference for hydrological drought management. The more weight is given to hydrological droughts, the more protection structures are applied in the main course of the Cesar River (Fig. 9e and f PDMM-6).

In solutions *a* and *b*, storage ponds allocate in the subbasins showing high runoff potential (Fig. 9a and b PDMM-7). According to the analysis of the hydroclimatic parameters influencing droughts in the Cesar River

basin by Paez-Trujilo et al. (2023), low infiltration capacity in these subbasins is associated with the soil hydrological group and land use that limits the infiltration. Then, allocating storage ponds in these sub-basins appears to reduce drought exposure by collecting surface runoff and allowing more time for infiltration. In solutions with preference for hydrological drought management, the storage ponds are allocated in the main channel from the headwater to the basin outlet. A few ponds are observed in basin east and in the Serranía del Perijá foothills.
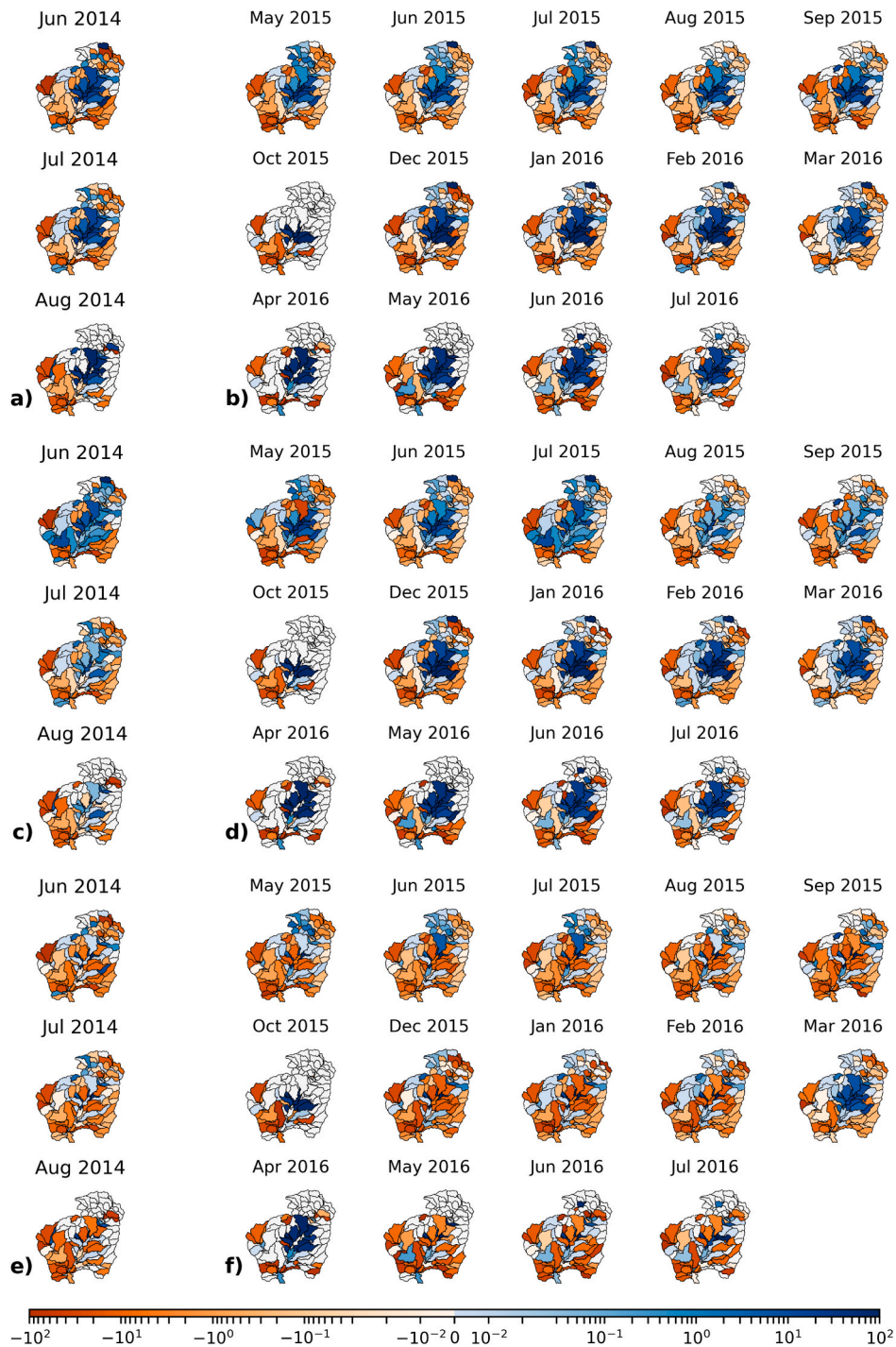

Fig. 10. Agricultural drought severity change in events V and VI for solutions *a*, *c*, and *f*. Solution *a* a) event V, b) event VI, solution *b* c) event V d) event VI, and solution *c* e) event V f) event VI.

4.4. Assessment of drought severity change by comparing drought severity in the baseline and the most-preferred trade-off solutions

The effect of PDMMs on the severity of agricultural and hydrological droughts was evaluated by comparing the drought severity in the baseline scenario to the drought severity in the selected solutions from the Pareto front. In the following, we describe the changes observed in the Pareto Front solutions *a*, *c* and *f*, in drought events V and VI.

4.4.1. Agricultural drought severity changes in solutions a, c and f

In solution *a*, the severity of agricultural droughts was reduced compared to the baseline scenario. This improvement was particularly notable in the northwest of the basin and the middle part of the river valley, especially during August 2014 (Fig. 10a), October 2015, December 2015 and January 2016 (Fig. 10b), with some subbasins experiencing a drought severity reduction of up to 100 %. The mitigation of the drought conditions in the river valley suggests that in solution *a*, the soil moisture water content increased by up to 20 mm (soil moisture deficit observed in the baseline scenario, Fig. 5a and b), and the agricultural drought ceased to occur during these months.

Agricultural drought alleviation was also observed in the subbasins experiencing the most severe soil moisture deficits. For instance, during event VI, specifically in March 2016 soil moisture deficit in the middle part of the river valley climbed up to 60 mm (Fig. 5b). According to the results, in March 2016, solution *a* contributed to reducing the agricultural drought severity by up to 20 % in the middle part of the river valley (Fig. 10b). Similarly, change in the severity of agricultural drought manifested consistently across the wet and dry months, in the short and long duration events analysed, as depicted in Fig. 10a and b.

RHW ponds, plantation and row crops and woodlands were allocated in the subbasins where agricultural drought severity declined (Fig. 9a). The examination of the model outputs revealed that the drop in agricultural drought severity is linked to a decline in the surface runoff volume and sediment yield values. Both changes are commonly associated with adequate soil structure, which in turn improves soil water retention capacity and the soil water content.

In solution *c*, the severity of agricultural droughts decreased in the basin's northwest and the middle part of the river valley, as in solution *a*; however, the deficit reduction was lower in solution *c*. While solution *a* exhibited a substantial decline of up to 100 % in drought severity in solution *c*, it remained below 20 %, with most values not exceeding 10 %, as observed during event V in June and July 2014. Specifically, in solution *a*, agricultural drought severity was reduced by up to 70 % (Fig. 10a). In turn, in solution *c*, severity was reduced by <10 %, except for a few subbasins in the river valley showing drought severity decrease of up to 25 % (Fig. 10c). It is worth mentioning that, in solution *c*, the number of subbasins showing a reduction in the agricultural drought severity was higher compared to solution *a*, as seen in Fig. 10c and d (e. g. June 2014, July 2014, May 2015, August 2015 and September 2015). Results indicated that the magnitude of agricultural drought reduction declined in solution *c*; nevertheless, the area experiencing drought alleviation increased compared to solution *a*, particularly during the first months of both drought events analysed.

Conversely, agricultural drought severity intensified in solutions *a* and *c* in the basin's west and La Serranía del Perijá. Fig. 10a shows that in solution *a*, agricultural drought rose by up to 60 % in the basin's west and by up to 20 % in La Serranía del Perijá during event V. For instance, in solution *a*, agricultural drought severity increased by up to 60 % in the west tip of the basin during August 2014 (Fig. 10a), potentially representing an increase of approximately 20 mm in the soil moisture deficit compared to the baseline scenario. In event VI, another considerable sure was observed in the basin's southwest. The agricultural drought severity consistently grew in this area by up to 70 % in May and June (Fig. 10b). This enhancement of the agricultural drought could correspond to an increase in the soil moisture deficit of approximately 10 mm compared to the baseline scenario. Interestingly, in the same

area, the rise in agricultural drought severity by 15 % in March 2016 could represent a leap in the soil moisture deficit of a similar magnitude (10 mm) compared to the baseline scenario.

Model results suggest that converting pastures (current land use) to row crops increased the surface runoff, and replacing pastures for plantation crops increased evapotranspiration in the subbasins where crops were allocated, leading to water loss through surface runoff and evapotranspiration and subsequently enhancing the soil moisture deficit.

In contrast to solutions *a* and *c*, agricultural drought severity primarily increased in solution *f*, with rare exceptions. In event V, the soil moisture deficit climbed up to 70 % in August 2104 (Fig. 10e). This increase could represent an enhancement of >35 mm for the soil moisture deficit in the western part of the basin. Regarding event VI, very little alleviation was observed, as shown in Fig. 10f. Agricultural drought severity reduction in the river valley appears more connected to the rainy period in March and April than the drought mitigating effect produced by the PDMMs. In 2015, drought severity decreased in May, June and July immediately after the precipitation events, and in 2016, drought severity only reduced in March and April. After the alleviation caused by the rainy season, drought severity surged in event VI; for instance, in August 2015, the severity increased by up to 50 % (Fig. 10f) in the river valley, potentially representing an increase of 40 mm in the soil moisture deficit compared to the baseline scenario.

Fig. 9a, c and f illustrate that PDMMs plots in solutions *a* and *c* are alike in the areas where the PDMMs allocate. Nevertheless, the application scale of plantation and row crops and woodland increases gradually from solution *a* to *f*, while the application of RWH ponds reduces. Accordingly, results indicate that the same PDMMs can mitigate or enhance one type of drought depending on the application scale of the intervention.

4.4.2. Hydrological drought severity changes in solutions a, c and f

Hydrological drought severity consistently increased across the wet and dry months in solution *a* (Fig. 11a and b). In the basin's headwater, an enhancement of the drought severity of up to 100 % was observed (event V, June 2014), with most values above 10 %. It is worth mentioning that the basin's north presented some of the highest drought deficits during the events analysed (e.g., June 2014, May and June 2015, Fig. 6a and b); thus, the drought severity growth represents approximately 1 mmd^{-1} increase in the streamflow deficit. On the other hand, hydrological drought alleviation in October and November (Fig. 11b) is likely linked to the increased precipitation in these months rather than the implementation of PDMMs. Given that the main rainfall events in the basin occur between August and November, this precipitation is a more probable cause of the observed hydrological drought alleviation in solution *a*.

Model outputs revealed that surface runoff was reduced during both events analysed. It suggests that PDMMs increased soil water-holding capacity in solution *a*. However, a consequential outcome was a diminished contribution of surface runoff to streamflow during wet periods. Further, model results also showed that no significant change in the groundwater contribution to the streamflow was observed in the subbasins where the interventions were applied. Interestingly, although several interventions were applied in the channels, they did not produce a significant drought severity alleviation, confirming that the efficiency of these interventions depends on the volume of water reaching the streamflow.

In solution *c*, a positive change in the severity of hydrological droughts was observed in the basins's west and La Serranía del Perijá. In contrast, hydrological drought tends to increase in the headwater and the river valley (Fig. 11c and d). In event VI, severity markedly reduced during the wet months (October and November), and the decline continued to occur for three months more (Fig. 11d). In the wet months, hydrological drought severity reduced up to 100 %, while in the subsequent months, dry months, up to 30 %. Fig. 10c and d and Fig. 11c and
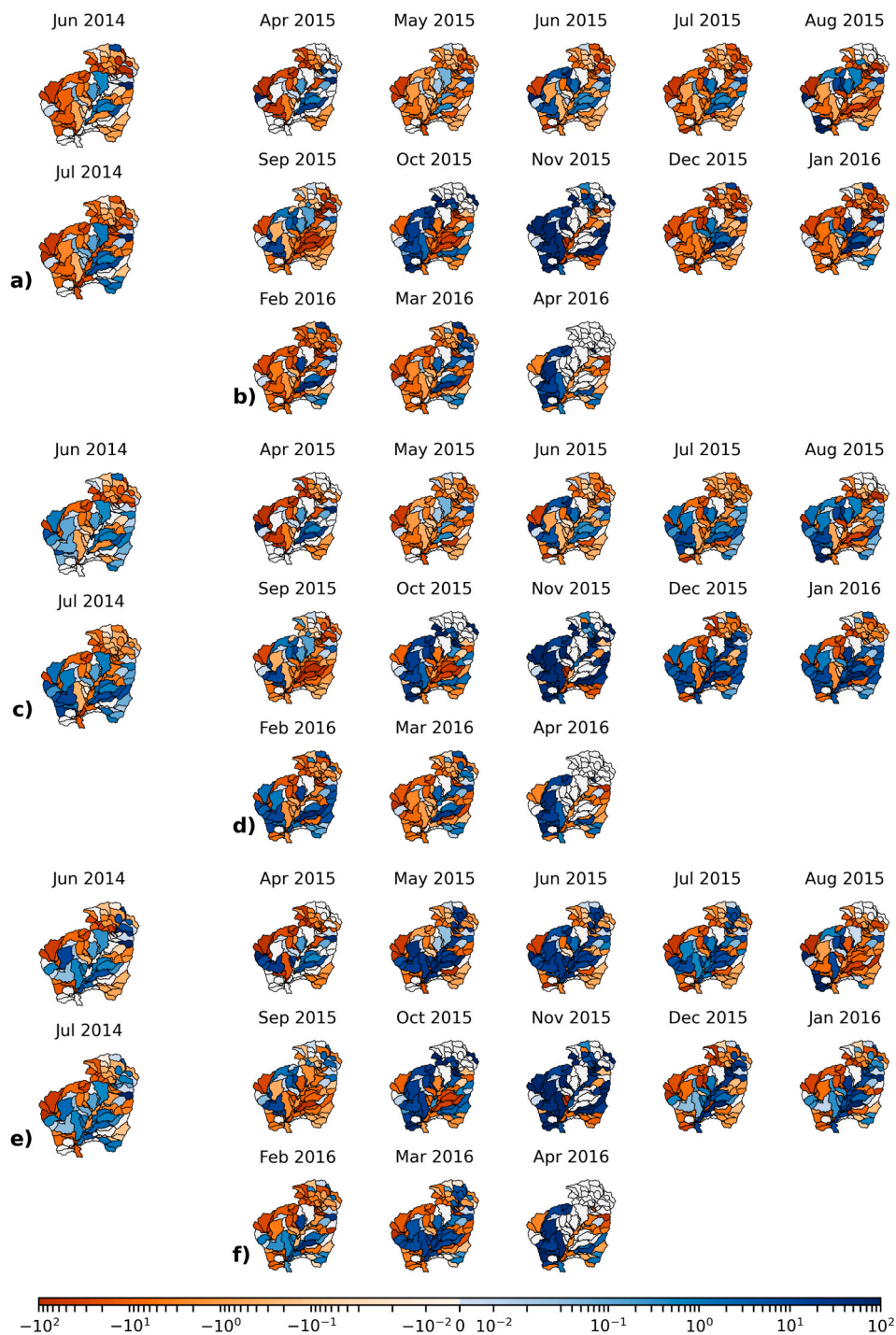
Fig. 11. Hydrological drought severity change in events V and VI for solutions *a*, *c*, and *f*. Solution *a* a) event V, b) event VI, solution *c* c) event V d) event VI, and solution *f* e) event V f) event VI.

d show that in the areas where agricultural drought severity decreased, hydrological drought severity worsened and vice-versa. It is relevant to mention that solution *c* exhibited one of the highest densities of PDMMs allocated. However, the alleviation of the two types of droughts is lower compared to the drought alleviation in the best solution for each type. This implies that a considerable number of PDMMs are required to satisfy both management objectives; however, the water input (mainly represented by precipitation) seems insufficient to meet both objectives, constraining the intervention's performance.

In solution *f*, hydrological drought severity consistently decreased in the river valley; alleviation extended from the headwater to the basin outlet during both events analysed (Fig. 11e and f). Alleviation of the hydrological drought severity in the river valley suggests that in solution *f*, the streamflow increased by up to 0.4 mmd^{-1} (hydrological drought severity observed in the baseline scenario, Fig. 6a and b). It should be noted that, in event V, the severity in the subbasins showing the highest streamflow deficits did not decrease (June and July 2014, Sierra Nevada, Fig. 6a); on the contrary, the severity raised by 70 % (Fig. 11e). In turn, during event VI, solution *f* contributed to alleviate the deficit in some of the subbasins more impacted for the drought; for instance, in la Sierra Nevada the deficit of >0.6 mmd^{-1} declined by up to 80 % (September, October and November 2015, Fig. 11f). This positive

impact can be associated to the combined effect of the wet season between October and November and the PDMMs allocated in the area.

Fig. 11f illustrates that positive hydrological drought response is the result of PDMMs plot consisting of RWH ponds allocated in the strip (also observed in solutions *a* and *c*), plantation crops in the basin's north, row crops distributed all over the basin, and woodlands allocation in the upper part of La Serranía del Perijá, and channel protection and storage ponds in the river's main course from the headwater up to the basin outlet. This reveals that alleviating the severity of hydrological drought in the middle course of the river results from the combined effect of different PDMMs allocated over the entire basin. Locally PDMMs' allocation seems problematic. For example, the allocation of row crops aggravated the hydrological drought in the basin's north and west. Similarly, woodlands allocation in the upper part of La Serranía del Perijá enhanced the drought deficit in some of the subbasins where the intervention was allocated.

5. Discussion

5.1. Insights on the PDMMs performance reducing severity of droughts

The outcomes of our study confirm that applying PDMMs has the potential to reduce the severity of agricultural and hydrological droughts. Nevertheless, it demonstrates that selecting and allocating the PMDDs is a complex task since results indicate that managing agricultural and hydrological droughts are conflicting objectives. For instance, in solution *a,* applying RWH ponds, and land use change to plantation crops and woodlands alleviated the severity of agricultural droughts in the basin's northwest and the middle part of the river valley. These results are consistent with previous studies asserting that combined interventions (e.g., adequate crops allocation, conservation agriculture, storage ponds, bench terracing) have a significant effect on water balance components such as infiltration and soil water holding capacity (Palumbo Silva et al., 2023; Uniyal et al., 2020).

Agricultural drought alleviation contrasts with the increased hydrological drought severity in areas where agricultural drought severity is reduced. According to previous findings reported in the literature, surface runoff, soil water flow, and groundwater recharge tend to decrease after the conversion of grasslands to croplands or forests. The groundwater recharge decline occurs from factors such as lower and shallow pore connectivity, higher evapotranspiration rates, and the top soil texture; for example, clayey soils exhibit lower infiltration rates, limiting the groundwater recharge (Owuor et al., 2016). Hydrological drought reduced from the headwater to the basin outlet in the river valley, while agricultural drought increased in the same area. Then, the solutions analysed demonstrate that PDMMs application reduces the severity of agricultural droughts but may produce the opposite effect on the severity of hydrological droughts (or vice versa).

The above fits well with the results obtained by Cai et al. (2015). The authors presented an optimisation framework to select preventive and tactical measures for drought management under different climate scenarios. Although the authors did not assess the measures' effect on the drought severity (or another drought characteristic), they identified the trade-off relationship between maximising the crop yield (variable representing the agricultural drought) and maximising the low flows (variable representing the hydrological drought) They also concluded that the climate-change scenarios would aggravate the trade-offs due to more limited water resources availability.

Moreover, the PDMMs' effect can vary in time and space. In this study, variation in time may be linked to the rainy season. In the three solutions analysed, the most considerable drought severity change is observed during the rainy season. Drought alleviation lasts until the dry season and declines gradually until the wet season starts again. Our findings indicate that the performance of PDMMs balancing the water cycle relies on rainfall availability.

Regarding variation in space, PDMMs can be beneficial for one type

of drought in a specific area but produce the opposite effect in another sector. In solution *a,* converting pastures (current land use) to plantation crops alleviated the severity of agricultural droughts in the basin's northwest and the middle part of the river valley. However, the same interventions exacerbated the agricultural drought severity in the basin's west. This concurs well with earlier studies showing that well-maintained grasslands can exhibit higher infiltration values compared to the same soil under cultivation due to shallow-rooted systems and lower evapotranspiration rates (Basche and Delonge, 2019; Krishnaswamy et al., 2018; Robinson et al., 2022).

For hydrological droughts, locally applied interventions can maximise the drought situation in the area where the measure is applied but alleviate the drought condition in the surrounding or downstream areas, as observed in solution *f* with the allocation of row crops in the basin's west and woodlands application in the basin's southeast. In both cases, hydrological drought worsens in the subbasins where the interventions are applied and reduced downstream. It poses an additional challenge to the implementation of PDMMs, considering the positive impact of the interventions may not be reflected in the areas where the intervention is applied.

Our findings indicate that PDMMs must be tailored to each region, and its planning requires careful assessment of the basin characteristics (e.g., rainfall distribution over the year, soil properties, current land use, and topography) and the drought characteristics and likelihood. Equally important, PDMMs' performance in reducing the severity of each type of drought should be quantified and monitored. This requires introducing appropriate indicators or criteria to measure PDMMs' effectiveness in alleviating droughts. All the above confirms that incremental, autonomous adjustments made by farmers and reactive measures taken by governments and institutions after drought emergencies are not the best and most effective strategies for long-term drought management (Mapedza and McLeman, 2019).

5.2. Insights on using optimisation for PDMMs planning

The obtained solutions corroborate the benefit of using multi-objective optimisation for PDMMs planning. Despite the significant number of decision variables, the algorithm progressed towards a near-to-optimal set of solutions, namely multiple drought management scenarios, including different PDMMs aiming to balance land and water phases of the hydrological cycle and reduce the severity of agricultural and hydrological droughts. In the context of drought management, the optimisation engine can be seen as a decision support tool applicable to identifying the most appropriate areas to implement PDMMs and estimate their impacts on the basin's hydrology. Even more, the solutions in the Pareto Front allow decision-makers to assess the trade-off between managing agricultural and hydrological droughts.

In this study, the most significant alleviation for both types of droughts is observed in the river's middle course. This is consistent with the formulation of the objective functions, which aggregate the values of the variables representing each type of drought at each HRU or subbasin. The river middle course presents the highest values of soil moisture and streamflow; thus, variable changes in that area tend to impact the objective functions more. In the areas where the variables representing agricultural and hydrological droughts are relatively lower, or the aridity index decreases (ratio between the precipitation and the evapotranspiration), drought severity alleviation is mainly observed in the best solutions for each type of drought. Weights can be assigned to underrepresented areas, preventing uneven contribution to the computation objective functions.

6. Conclusion

In this study, we framed the task of selecting and allocating preventive drought management measures (PDMMs) as an optimisation problem. Accordingly, we integrated the Soil Water Assessment Tool

(SWAT) modelling system and the Unified Evolutionary Algorithm for Single, Multiple, and Many-Objective Optimization (U-NSGA-III) to develop an optimisation engine for planning PDMMs. The optimisation approach allows the representation of seven PDDMs, namely RWH ponds, plantation and row crops allocation, woodlands allocation, channel protection, grade control and storage ponds within various management scenarios (solutions) and simulation of their impact on the soil moisture and the streamflow, variables used to represent agricultural and hydrological droughts. Then, we assessed the PMDMs' performance in mitigating droughts, comparing the agricultural and hydrological drought severity in the baseline scenario to the severity in selected drought management scenarios.

The findings from our study confirm that implementing PDMMs has the potential to reduce the severity of agricultural and hydrological droughts, and the obtained management scenarios (solutions) underscore the utility of multi-objective optimisation for PDMMs planning. Analysed scenarios reveal that PDMMs can reduce the severity of agricultural droughts while producing the opposite effect for hydrological droughts (or vice versa). Moreover, the impact of PDMMs exhibits temporal and spatial variations. PDMMs implemented in a particular subbasin may ameliorate the severity of one type of drought in a particular month but worsen the drought situation in the preceding or coming months. In the case of hydrological droughts, the measures can intensify the streamflow deficit in the subbasins where the interventions are allocated while reducing the hydrological downstream (or vice versa). In light of all this, PDMMs should be tailored to each region, and its planning requires careful assessment of the basin characteristics (e.g., rainfall distribution over the year, soil properties, current land use, and topography) and prior assessment of PDMMs' applicability to reducing the severity of each type of drought.

This study is not exempt from certain limitations. Firstly, future work may assess the non-stationarity in the soil moisture and streamflow time series. If non-stationarity is confirmed, it will be necessary to identify the most appropriate technique to transform the time series before calculating the empirical distribution function and the drought thresholds. Secondly, further work is needed to refine the representation of PDMMs and their effect on the hydrological cycle and droughts' severity. Specifically, crops and woodlands allocation requires improving the representation of vegetation growth, given that the temperature-based approach incorporated in SWAT has been found to have limitations in tropical regions (Abitew et al., 2023). Additionally, a more detailed crop management schedule is needed to simulate better crops' growth influence on the water balance of cultivated areas. Thirdly, the practical implementation of PDMMs involves substantial investments; therefore, further extensions of this work may evaluate cost-effective management scenarios incorporating an objective function that accounts for costs associated with PDMMs implementation. Even more, minimising hydrological drought severity implies streamflow increase; future work may include a flood-associated constraint that prevents the potential incidence of floods in the wet season, particularly in the solutions with a preference for hydrological droughts.

Lastly, this study relied exclusively on a single optimization algorithm, U-NSGA-III, for defining and testing the optimisation engine. Subsequent research should explore the incorporation of alternative algorithms. This is a recommended practice to assess algorithms' effectiveness, efficiency and reliability (Maskey et al., 2002; Solomatine, 1998).

Funding

Ethics approval

Not applicable.

Consent to participate

Not applicable.

Consent for publication

There is no conflict of interest regarding the publication of this article.

CRediT authorship contribution statement

Ana M. Paez-Trujillo: Writing – original draft, Methodology, Investigation, Funding acquisition, Conceptualization. **J. Sebastian Hernandez-Suarez:** Writing – original draft, Methodology, Conceptualization. **Leonardo Alfonso:** Writing – review & editing, Conceptualization. **Beatriz Hernandez:** Writing – review & editing. **Shreedhar Maskey:** Writing – review & editing, Methodology, Conceptualization. **Dimitri Solomatine:** Writing – review & editing.

Declaration of competing interest

The authors declare that they have no known competing financial interests or personal relationships that could have appeared to influence the work reported in this paper.

Data availability

Data will be made available on request.

Acknowledgements

References

Abbasi, N.A., Xu, X., Lucas-Borja, M.E., Dang, W., Liu, B., 2019. The use of check dams in watershed management projects: examples from around the world. Sci. Total Environ. 676, 683–691. https://doi.org/10.1016/J.SCITOTENV.2019.04.249.

Abitew, T.A., Arnold, J., Jeong, J., Jones, A., Srinivasan, R., 2023. Innovative approach to prognostic plant growth modeling in SWAT+ for forest and perennial vegetation in tropical and sub-tropical climates. J. Hydrol. X 20, 100156. https://doi.org/10.1016/J.HYDROA.2023.100156.

Agencia de Desarrollo Rural, FAO, Gobernacion del Cesar, 2019. Plan integral de desarrollo agropecuario y rural con enfoque territorial. TOMO II, Valledupar.

Akpoti, K., Kabo-Bah, A.T., Zwart, S.J., 2019. Agricultural land suitability analysis: State-of-the-art and outlooks for integration of climate change analysis. https://doi.org/10.1016/j.agsy.2019.02.013.

Arnold, J.G., Moriasi, D.N., Gassman, P.W., Abbaspour, K.C., White, M.J., Srinivasan, R., Santhi, C., Harmel, R.D., Van Griensven, A., Van Liew, M.W., Kannan, N., Jha, M.K., Harmel, D., Member, A., Van Liew, Michael W., Arnold, J.-F.G., 2012. SWAT: model use, calibration, and validation. Trans. ASABE 55, 1491–1508.

Assimacopoulos, D., Kampragou, E., Andreu, J., Bifulco, C., de Carli, A., De Stefano, L., Dias, S., Kartalidis, A., Massarutto, A., Monteagudo, D., Wolters, W., et al., 2015. Drought risk mitigation options–case study scale.

Auger, A., Bader, J., Brockhoff, D., Zitzler, E., 2012. Hypervolume-based multiobjective optimization: theoretical foundations and practical implications. Theor. Comput. Sci. 425, 75–103. https://doi.org/10.1016/J.TCS.2011.03.012.

Basche, A., 2017. Turning soils into sponges how farmers can fight floods and droughts [WWW document]. Union of concerned scientists. URL www.ucsusa.org/SoilsIntoSponges.

Basche, A., Delonge, M., 2019. Comparing infiltration rates in soils managed with conventional and alternative farming methods: A meta-analysis. https://doi.org/10.1371/journal.pone.0215702.

Beets, P.N., Beets, J.M., 2020. Soil water storage changes in a small headwater catchment in the central North Island of New Zealand following afforestation with Pinus radiata. For. Ecol. Manage. 462 https://doi.org/10.1016/j.foreco.2020.117967.

Bhat, S.A., Hussain, I., Huang, N.-F., 2023. Soil suitability classification for crop selection in precision agriculture using GBRT-based hybrid DNN surrogate models. Ecol. Inform. 75, 102109 https://doi.org/10.1016/j.ecoinf.2023.102109.

Blank, J., Deb, K., 2020. Pymoo: multi-objective optimization in python. IEEE Access 8, 89497–89509. https://doi.org/10.1109/ACCESS.2020.2990567.

Blank, J., Deb, K., Dhebar, Y., Bandaru, S., Seada, H., 2021. Generating well-spaced points on a unit simplex for evolutionary many-objective optimization. IEEE Trans. Evol. Comput. 25, 48–60. https://doi.org/10.1109/TEVC.2020.2992387.

Brunner, M.L., Swain, D.L., Gilleland, E., Wood, A.W., 2021. Increasing importance of temperature as a contributor to the spatial extent of streamflow drought. Environ. Res. Lett. 16 https://doi.org/10.1088/1748-9326/abd2f0.

Cai, X., Asce, M., Zeng, R., Won, Kang, H., Song, J., Valocchi, A.J., 2015. Strategic planning for drought mitigation under climate change. J. Water Resour. Plan. Manag. 141 https://doi.org/10.1061/(ASCE)WR.1943-5452.0000510.

Carrão, H., Naumann, G., Barbosa, P., 2018. Global projections of drought hazard in a warming climate: a prime for disaster risk management. Climate Dynam. 50, 2137–2155. https://doi.org/10.1007/s00382-017-3740-8.

Ciotti, D.C., Mckee, J., Pope, K.L., Kondolf, G.M., Pollock, M.M., 2021. Design criteria for process-based restoration of fluvial systems. Bioscience 71, 831–845. https://doi.org/10.1093/biosci/biab065.

Cottrell, R.S., Nash, K.L., Halpern, B.S., Remenyi, T.A., Corney, S.P., Fleming, A., Fulton, E.A., Hornborg, S., Johne, A., Watson, R.A., Blanchard, J.L., 2019. Food production shocks across land and sea. Nature Sustainability 2019 (2), 130–137. https://doi.org/10.1038/s41893-018-0210-1.

DANE, 2019. Encuesta nacional agropecuaria (ENA) [WWW Document]. URL https://www.dane.gov.co/index.php/estadisticas-por-tema/agropecuario/encuesta-naciona l-agropecuaria-ena (accessed 11.28.23).

Deb, K., 2001. Multi-Objective Optimization Using Evolutionary Algorithms. John Wiley & Sons, New York, NY, USA.

Deb, K., Lu, Z., Kropp, I., Hernandez-Suarez, J.S., Hussein, R., Miller, S., Nejadhashemi, A.P., 2023. Minimizing expected deviation in upper level outcomes due to lower level decision making in hierarchical multiobjective problems. IEEE Transactions on Evolutionary Computation 27, 505–519. https://doi.org/10.1109/TEVC.2022.3172302.

Du, B., Arnold, J.G., Saleh, A., Jaynes, D.B., 2005. Development and application of SWAT to landscapes with tiles and potholes. Trans. Am. Soc. Agric. Eng. 48, 1121–1133. https://doi.org/10.13031/2013.18522.

Duel, H., Henk, W., Ingrid, T., ter Maat, Judith, John, M., 2022. HELP Guiding Principles for Drought Risk Management under a Changing Climate Catalysing actions for enhancing climate resilience.

Dutch National Supercomputer Snellius, 2023. Dutch National Supercomputer Snellius | SURF.Nl [WWW document]. URL https://www.surf.nl/en/dutch-national-super computer-snellius.

FAO, 2019. Proactive Approaches to Drought Preparedness – Where Are We Now and Where Do We Go From Here? Rome.

GEF, BID, Fundación Natura, 2020. Proyecto manejo sostenible y conservacion de la biodiversidad en la cuenca del Río Magdalena. Modelo hidrológico refinado 1 en la cuenca del Río Cesar.

GEF, BID, Fundación Natura, 2021. Proyecto manejo sostenible y conservacion de la biodiversidad en la cuenca del Río Magdalena. Modelo hidrológico refinado 2 en la cuenca del Río Cesar.

Geng, R., Yin, P., Sharpley, A.N., 2019. A coupled model system to optimize the best management practices for nonpoint source pollution control. https://doi.org/10.1016/j.jclepro.2019.02.127.

Gerber, N., Mirzabaev, A., 2017. Benefits of Action and Costs of Inaction: Drought Mitigation and Preparedness - a Literature Review. Geneva, Switzerland and GWP, Stockholm, Sweden.

Global Water Partnership Central and Eastern Europe, 2015. Guidelines for Preparation of the Drought Management Plans. Development and Implementation in the Context of the EU Water Framework Directive. Global Water Partnership Central and Eastern Europe.

Gómez, A.M., Parra, A., Pavelsky, T.M., Wise, E., Villegas, J.C., Meijide, A., 2023. Ecohydrological impacts of oil palm expansion: a systematic review. Environ. Res. Lett. 18, 033005 https://doi.org/10.1088/1748-9326/ACBC38.

Greene, R.H., Thoms, M.C., Parsons, M., 2023. We cannot turn back time: a framework for restoring and repairing rivers in the Anthropocene. Front. Environ. Sci. 11 https://doi.org/10.3389/fenvs.2023.1162908.

Haile, G.G., Tang, Q., Li, W., Liu, X., Zhang, X., 2020. Drought: Progress in broadening its understanding. Wiley Interdisc. Rev. Water 7, e1407. https://doi.org/10.1002/WAT2.1407.

Heidari, A., Mayer, A., Watkins, D., Castillo, M.M., 2020. Hydrologic impacts and trade-offs associated with developing oil palm for bioenergy in Tabasco. Mexico. J Hydrol Reg Stud 31, 100722. https://doi.org/10.1016/J.EJRH.2020.100722.

Hernandez-Suarez, J.S., Nejadhashemi, A.P., 2022. Probabilistic predictions of ecologically relevant hydrologic indices using a hydrological model. Water Resour. Res. 58 https://doi.org/10.1029/2021WR031104 e2021WR031104.

Herrera-Estrada, J.E., Satoh, Y., Sheffield, J., 2017. Spatiotemporal dynamics of global drought. Geophys. Res. Lett. 44, 2254–2263. https://doi.org/10.1002/2016GL071768.

Heudorfer, B., Stahl, K., 2017. Comparison of different threshold level methods for drought propagation analysis in Germany. Hydrol. Res. 48, 1311–1326. https://doi.org/10.2166/nh.2016.258.

Hildemann, M., Pebesma, E., Verstegen, J.A., 2023. Multi-objective allocation optimization of soil conservation measures under data uncertainty. Environ. Manag. https://doi.org/10.1007/s00267-023-01837-6.

Hisdal, H., Tallaksen, L.M., Gauster, T., Bloomfield, J.P., Parry, S., Prudhomme, C., Wanders, N., 2024. Hydrological drought characteristics. In: Hydrological Drought. Elsevier, pp. 157–231. https://doi.org/10.1016/B978-0-12-819082-1.00006-0.

Huang, Z., Nya, E.L., Rahman, M.A., Mwamila, T.B., Cao, V., Gwenzi, W., Noubactep, C., 2021. Integrated water resource management: rethinking the contribution of rainwater harvesting. Sustainability (Switzerland) 13. https://doi.org/10.3390/su13158338.

Iglesias, A., Assimacopoulos, D., Van Lanen, H.A.J. (Eds.), 2018. Drought: Science and Policy. John Wiley & Sons, Incorporated. https://doi.org/10.1002/9781119017073.ch1.

Inamdar, S.P., Kaushal, S.S., Tetrick, R.B., Trout, L., Rowland, R., Genito, D., Bais, H., 2023. More than dirt: soil health needs to be emphasized in stream and floodplain restorations. Soil Syst 7. https://doi.org/10.3390/soilsystems7020036.

Instituto de hidrología meteorología y estudios ambientales (IDEAM), 2019. Estudio Nacional del Agua 2018. Bogotá.

Instituto Geografico Agustin Codazzi, Corporacion Autonoma Regional del Cesar, 2018. Estudio general de suelos y zonificación de tierras. Departamento del Cesar. Escala: 1:100.000. Bogota.

Jalowska, A.M., Yuan, Y., 2019. Evaluation of SWAT impoundment modeling methods in water and sediment simulations. J. Am. Water Resour. Assoc. 55, 209–227. https://doi.org/10.1111/1752-1688.12715.

Jones, J., Ellison, D., Ferraz, S., Lara, A., Wei, X., Zhang, Z., 2022. Forest restoration and hydrology. For. Ecol. Manage. 520 https://doi.org/10.1016/j.foreco.2022.120342.

de Jong van Lier, Q., Logsdon, S.D., Pinheiro, E.A.R., Gubiani, P.I., 2023. Plant available water. Encyclopedia of Soils in the Environment 509–515. https://doi.org/10.1016/B978-0-12-822974-3.00043-4.

Kahinda, J.M., Lillie, E.S.B., Taigbenu, A.E., Taute, M., Boroto, R.J., 2008. Developing suitability maps for rainwater harvesting in South Africa. https://doi.org/10.1016/j.pce.2008.06.047.

King-Okumu, C., 2021. A rapid review of drought risk mitigation measures – integrated drought management. Rome. https://doi.org/10.4060/cb7085en.

Krishnaswamy, J., Kelkar, N., Birkel, C., 2018. Positive and neutral effects of forest cover on dry-season stream flow in Costa Rica identified from Bayesian regression models with informative prior distributions. Hydrol. Process. 32, 3604–3614. https://doi.org/10.1002/HYP.13288.

Lewis, A., Randall, M., 2017. Solving multi-objective water management problems using evolutionary computation. https://doi.org/10.1016/j.jenvman.2017.08.044.

Li, M.-H., Eddleman, K.E., 2002. Biotechnical engineering as an alternative to traditional engineering methods a biotechnical streambank stabilization design approach. Landsc. Urban Plan. 60, 225–242.

Liu, G., Chen, L., Wei, G., Shen, Z., 2019. New framework for optimizing best management practices at multiple scales. https://doi.org/10.1016/j.jhydrol.2019.124133.

Liu, L., Dobson, B., Mijic, A., 2023. Optimisation of urban-rural nature-based solutions for integrated catchment water management. J. Environ. Manage. 329, 117045 https://doi.org/10.1016/J.JENVMAN.2022.117045.

Lucas-Borja, M.E., Piton, G., Yu, Y., Castillo, C., Antonio Zema, D., 2021. Check dams worldwide: objectives, functions, effectiveness and undesired effects. Catena (Amst) 204, 105390. https://doi.org/10.1016/J.CATENA.2021.105390.

Mapedza, Everisto, McLeman, R., 2019. Drought risks in developing regions: Challenges and opportunities. In: Mapedza, E., Tsegai, D., Bruntrup, M., Mcleman, R. (Eds.), Current Directions in Water Scarcity Research. Elsevier, pp. 1–14. https://doi.org/10.1016/B978-0-12-814820-4.00001-8.

Maskey, S., Jonoski, A., Solomatine, D.P., 2002. Groundwater remediation strategy using global optimization algorithms. J Water Resour Plan Manag 128. https://doi.org/10.1061/ASCE0733-94962002128:6431.

Moriasi, D.N., Arnold, J.G., Van Liew, Bingner, R.L., Harmel, R.D., Veith, T.L., 2007. Model evaluation guidelines for systematic quantification of accuracy in watershed simulations. Trans. ASABE 50, 885–900. https://doi.org/10.13031/2013.23153.

Mosleh, Z., Salehi, M.H., Fasakhodi, A.A., Jafari, A., Mehnatkesh, A., Borujeni, I.E., 2017. Sustainable allocation of agricultural lands and water resources using suitability analysis and mathematical multi-objective programming. https://doi.org/10.1016/j.geoderma.2017.05.015.

Muhar, S., Sendzimir, Jan, Jungwirth, M., Hohensinner, S., 2018. Restoration in integrated river basin management. In: Schmutz, S., Sendzimir, J. (Eds.), Riverine Ecosystem Management. Aquatic Ecology Series, vol. 8. Springer, Cham. https://doi.org/10.1007/978-3-319-73250-3_15.

Naseri, F., Azari, M., Dastorani, M.T., 2021. Spatial optimization of soil and water conservation practices using coupled SWAT model and evolutionary algorithm. International Soil and Water Conservation Research 9, 566–577. https://doi.org/10.1016/j.iswcr.2021.04.002.

Natural Resources Conservation Service, 2007. Grade Stabilization Techniques. In: National Engineering Handbook.

Neitsch, S.L., Arnold, J.G., Kiniry, J.R., Williams, J.R., 2011. Soil and Water Assessment Tool Theoretical Documentation Version 2009 Texas Water Resources Institute. Texas Water Resources Institute.

Nyagumbo, I., Nyamadzawo, G., Mapembo, C., 2019. Effects of three in-field water harvesting technologies on soil water content and maize yields in a semi-arid region of Zimbabwe. https://doi.org/10.1016/j.agwat.2019.02.023.

Oweis, T.Y., Prinz, D., Hachum, A.Y., 2012. Rainwater Harvesting for Agriculture in the Dry Areas, Rainwater Harvesting for Agriculture in the Dry Areas. CRC Press. https://doi.org/10.1201/b12351.

Owuor, S.O., Butterbach-Bahl, K., Guzha, A.C., Rufino, M.C., Pelster, D.E., Díaz-Pinés, E., Breuer, L., 2016. Groundwater recharge rates and surface runoff response to land use and land cover changes in semi-arid environments. Ecol. Process. 5, 1–21. https://doi.org/10.1186/S13717-016-0060-6/TABLES/4.

Pacheco, F.A.L., Van Der Weijden, C.H., 2014. Modeling rock weathering in small watersheds. https://doi.org/10.1016/j.jhydrol.2014.03.036.

Paez-Trujilo, A., Cañon, J., Hernandez, B., Corzo, G., Solomatine, D., 2023. Multivariate regression trees as an "explainable machine learning" approach to explore relationships between hydroclimatic characteristics and agricultural and hydrological drought severity: case of study Cesar River basin. Nat. Hazards Earth Syst. Sci. 23, 3863–3883. https://doi.org/10.5194/NHESS-23-3863-2023.

Palumbo Silva, T., Bressiani, D., Diniz Ebling, E., Miguel Reichert, J., . Best management practices to reduce soil erosion and change water balance components in watersheds under grain and dairy production-NC-ND license. http://creativecommons.org/licenses/by-nc-nd/4.0/. https://doi.org/10.1016/j.iswcr.2023.06.003.

Piemontese, L., Castelli, G., Fetzer, I., Barron, J., Liniger, H., Harari, N., Bresci, E., Jaramillo, F., 2020. Estimating the global potential of water harvesting from successful case studies. https://doi.org/10.1016/j.gloenvcha.2020.102121.

Pinto, A., Sanches Fernandes, L.F., Maia, R., Fernandes, L.F.S., 2016. Monitoring methodology of interventions for riverbanks stabilization: assessment of technical solutions performance. Water Resour. Manag. 30 https://doi.org/10.1007/s11269-016-1486-4.

Pischke, F., Stefanski, R., 2017. Integrated Drought Management Initiatives, in: Drought and Water Crises Integrating Science, Management, and Policy. CRC. https://doi.org/10.1201/b22009.

Rabelo, U.P., Dietrich, J., Costa, A.C., Simshäuser, M.N., Scholz, F.E., Nguyen, V.T., Lima Neto, I.E., 2021. Representing a dense network of ponds and reservoirs in a semi-distributed dryland catchment model. J Hydrol (Amst) 603. https://doi.org/10.1016/j.jhydrol.2021.127103.

Rabot, E., Wiesmeier, M., Schlüter, S., Vogel, H.-J., 2017. Soil structure as an indicator of soil functions: A review. https://doi.org/10.1016/j.geoderma.2017.11.009.

Rachmawati, L., Srinivasan, D., 2009. Multiobjective evolutionary algorithm with controllable focus on the knees of the pareto front. IEEE Transactions on Evolutionary Computation 13, 810–824. https://doi.org/10.1109/TEVC.2009.2017515.

Raschke, A., Hernandez-Suarez, J.S., Nejadhashemi, A.P., Deb, K., 2021. Multidimensional aspects of sustainable biofuel feedstock production. Sustainability 13, 1424. https://doi.org/10.3390/SU13031424.

Robinson, D.A., Nemes, A., Reinsch, S., Radbourne, A., Bentley, L., MKeith, A.M., 2022. Global meta-analysis of soil hydraulic properties on the same soils with differing land use. Sci. Total Environ. 852 https://doi.org/10.1016/j.scitotenv.2022.158506.

Rosgen, D.L., 2001. The cross-vane, W-weir and J-hook vane structures…their description, design and application for stream stabilization and river restoration. In: Wetlands Engineering & River Restoration 2001. American Society of Civil Engineers, Reston, VA, pp. 1–22. https://doi.org/10.1061/40581(2001)72.

Sanz, M.J., de Vente, J., Chotte, J.-L., Bernoux, M., Kust, G., Ruiz, I., 2017. Sustainable Land Management Contribution to Successful Land-Based Climate Change Adaptation and Mitigation.

Sayers, P.B., Yuanyuan, L., Moncrieff, C., Jianqiang, L., Tickner, D., Gang, L., Speed, R., 2017. Strategic drought risk management: eight 'golden rules' to guide a sound approach. Int. J. River Basin Manag. 15, 239–255. https://doi.org/10.1080/15715124.2017.1280812.

Seada, H., Deb, K., 2016. A unified evolutionary optimization procedure for single, multiple, and many objectives. IEEE Transactions on Evolutionary Computation 20, 358–369. https://doi.org/10.1109/TEVC.2015.2459718.

Sheffield, F., Wood, E.F., 2011. What is drought. In: Drought: Past Problems and Future Scenarios. Taylor & Francis Group, pp. 9–15.

Solomatine, D.P., 1998. Genetic and other global optimization algorithms-comparison and use in calibration problems. In: Proc.3rdInternationalConferenceonHydroinformatics. Copenhagen, pp. 1021–1028.

Tallaksen, L.M., Hisdal, H., Lanen, H.A.J.V., 2009. Space-time modelling of catchment scale drought characteristics. J Hydrol (Amst) 375, 363–372. https://doi.org/10.1016/j.jhydrol.2009.06.032.

Terêncio, D.P.S., Sanches Fernandes, L.F., Cortes, R.M.V., Pacheco, F.A.L., 2017. Improved framework model to allocate optimal rainwater harvesting sites in small watersheds for agro-forestry uses. https://doi.org/10.1016/j.jhydrol.2017.05.003.

Tsegai, D., Stefanski, R., Mejias Moreno Author, P., Tadesse, T., 2018. Strategic framework for drought risk managementand enhancing resilience in Africa.

UNCCD, 2019. The Land-Drought Nexus Enhancing the Role of Land-Based Interventions in Drought Mitigation and Risk Management.

UNCCD, 2022. Drought in Numbers 2022 - Restoration for Readiness and Resilience.

UNDRR, 2021. GAR Special Report on Drought 2021. Geneva.

Universidad del Atlantico, 2014. Plan de ordenamiento del recurso hidrico del Rio Cesar Formulacion Final.

Uniyal, B., Jha, M.K., Kumar Verma, A., Anebagilu, P.K., 2020. Identification of critical areas and evaluation of best management practices using SWAT for sustainable watershed management. Sci. Total Environ. 744, 140737 https://doi.org/10.1016/j.scitotenv.2020.140737.

Vicente-Serrano, S.M., Quiring, S.M., Peña-Gallardo, M., Yuan, S., Domínguez-Castro, F., 2020. A review of environmental droughts: increased risk under global warming? Earth Sci. Rev. 201 https://doi.org/10.1016/J.EARSCIREV.2019.102953.

Vogt, J.V., Naumann, G., Masante, D., Spinoni, J., Cammalleri, C., Erian, W., Pischke, F., Pulwarty, R., Barbosa, P., 2018. Drought Risk Assessment and Management. A Conceptual Framework. Luxembourg. https://doi.org/10.2760/057223.

Waidler, D., White, M., Steglich, E., Wang, S., Williams, J., Jones, C.A., Srinivasan, R., 2009. Conservation Practice Modeling Guide for SWAT and APEX.

Wambura, F.J., Dietrich, O., Graef, F., 2018. Analysis of infield rainwater harvesting and land use change impacts on the hydrologic cycle in the Wami River basin. Agric Water Manag 203, 124–137. https://doi.org/10.1016/j.agwat.2018.02.035.

Wang, J.M., Yang, X.G., Zhou, H.W., Wang, Z.H., Zhou, J.W., Liang, Y.F., 2017. The effect of tetrahedron framed permeable weirs on river bed stability in a mountainous area under clear water conditions. Scientific Reports 1–14. https://doi.org/10.1038/s41598-017-04711-8, 2017 7:1 7.

Wang, T., Hou, J., Li, Peng, Zhao, J., Li, Z., Matta, E., Ma, Liping, Hinkelmann, Reinhard, 2021. Quantitative assessment of check dam system impacts on catchment flood characteristics – a case in hilly and gully area of the loess plateau, China. Nat. Hazards 105, 3059–3077. https://doi.org/10.1007/s11069-020-04441-7.

Wilhite, D.A., 2016. Drought-Management Policies and Preparedness Plans: Changing the Paradigm from Crisis to Risk Management. In: Land Restoration. Elsevier, pp. 443–462. https://doi.org/10.1016/B978-0-12-801231-4.00007-0.

Wilhite, D.A., 2019. Integrated drought management: moving from managing disasters to managing risk in the Mediterranean region. EuroMediterr J Environ Integr 4, 1–5. https://doi.org/10.1007/S41207-019-0131-Z/FIGURES/2.

Wohl, E., Lane, S.N., Wilcox, A.C., 2015. The science and practice of river restoration. Water Resour. Res. 51, 5974–5997. https://doi.org/10.1002/2014WR016874.

Woodward, M., Gouldby, B., Kapelan, Zoran, Hames, D., 2014. Multiobjective Optimization for Improved Management of Flood Risk. https://doi.org/10.1061/(ASCE).

World Bank, 2019. Assessing Drought Hazard and Risk: Principles and Implementation Guidance. Washington, DC.

Wu, H., Zhu, A.X., Liu, J., Liu, Y., Jiang, J., 2018. Best management practices optimization at watershed scale: incorporating spatial topology among fields. Water Resources Management 32, 155–177. https://doi.org/10.1007/s11269-017-1801-8.

Yadav, G.S., Saha, P., Babu, S., Das, A., Layek, J., Debnath, C., 2018. Effect of no-till and raised-bed planting on soil moisture conservation and productivity of summer maize (Zea mays) in eastern Himalayas. Agric. Res. 7, 300–310. https://doi.org/10.1007/s40003-018-0308-8.

Yevjevich, V., 1967. An objective approach to definitions and investigations of continental hydrologic droughts. J Hydrol (Amst) 7, 353. https://doi.org/10.1016/0022-1694(69)90110-3.

Zelenhasić, E., Salvai, A., 1987. A method of streamflow drought analysis. Water Resour. Res. 23, 156–168. https://doi.org/10.1029/WR023i001p00156.

Zhang, X., Hao, Z., Singh, V.P., Zhang, Y., Feng, S., Xu, Y., Hao, F., 2022. Drought propagation under global warming: characteristics, approaches, processes, and controlling factors. Sci. Total Environ. 838, 156021 https://doi.org/10.1016/J.SCITOTENV.2022.156021.

Zhang, Z., Montas, H., Shirmohammadi, A., Leisnham, P., Negahban-Azar, M., 2023. Effectiveness of BMP Plans in Different Land Covers, with Random, Targeted, and Optimized Allocation. https://doi.org/10.1016/j.scitotenv.2023.164428.